General Disclaimer

One or more of the Following Statements may affect this Document

- This document has been reproduced from the best copy furnished by the organizational source. It is being released in the interest of making available as much information as possible.

- This document may contain data, which exceeds the sheet parameters. It was furnished in this condition by the organizational source and is the best copy available.

- This document may contain tone-on-tone or color graphs, charts and/or pictures, which have been reproduced in black and white.

- This document is paginated as submitted by the original source.

- Portions of this document are not fully legible due to the historical nature of some of the material. However, it is the best reproduction available from the original submission.

NASA TECHNICAL MEMORANDUM NASA TM 75278

THE EXECUTION OF SYSTEMATIC MEASUREMENTS ON PLANE CASCADES

Norbert Scholz

(NASA-TM-75278) THE EXECUTION OF SYSTEMATIC MEASUREMENTS ON PLANE CASCADES (National Aeronautics and Space Administration) 56 p HC A04/MF A01 CSCL 20D

N78-21413

Unclas
G3/34 15900

Translation of "Über die Durchführung systematischer Messungen an ebenen Schaufelgittern", Zeitschrift fuer Flugwissenschaften, vol.4, no.10, October, 1956, pp. 313-333.

NATIONAL AERONAUTICS AND SPACE ADMINISTRATION
WASHINGTON, D. C. 20546 APRIL 1978

STANDARD TITLE PAGE

1. Report No.	2. Government Accession No.	3. Recipient's Catalog No.
NASA TM-75278		

4. Title and Subtitle	5. Report Date
THE EXECUTION OF SYSTEMATIC MEASUREMENTS ON PLANE CASCADES.	6. Performing Organization Code

7. Author(s)	8. Performing Organization Report No.
Norbert Scholz	10. Work Unit No.

9. Performing Organization Name and Address	11. Contract or Grant No.
SCITRAN 1482 East Valley Road, Box 5456 Santa Barbara, CA 93108	13. Type of Report and Period Covered

12. Sponsoring Agency Name and Address	14. Sponsoring Agency Code
National Aeronautics and Space Administration Washington, D. C., 20546	

15. Supplementary Notes

Translation of "Uber die Durchführung systematischer Messungen an ebenen Schaufelgittern", Zeitschrift fuer Flugwissenschaften, vol4, no10. October, 1956, pp. 313-333.

16. Abstract

Systematic measurements of flow through cascades: cascade wind tunnel developed by author at Institute for Fluid Mechanics at Technische Hochschule Braunschweig, described: equations developed for evaluation of momentum measurements in 2-dimensional flow through cascades. 24 refs.

17. Key Words (Selected by Author(s))	18. Distribution Statement

19. Security Classif. (of this report)	20. Security Classif. (of this page)	21. No. of Pages	22. Price
Unclass.	Unclass.	54	

THE EXECUTION OF SYSTEMATIC MEASUREMENTS ON PLANE CASCADES*

Norbert Scholz

ABSTRACT /313**

The present state of development of the experimental technique regarding the flow through cascades and several points to be specially observed in the design of cascade wind tunnels are discussed. The cascade wind tunnel developed by the author and used at the Institute for Fluid Mechanics at the Technical University of Braunschweig, is described.

The equations required for the evaluation of the momentum measurements in two-dimensional flow through cascades are developed. Applying a correction of general applicability, it is possible to convert the computation of the wake flow in a very simple manner. Regarding the effect of the jet contraction due to the boundary layer along the side walls a simple method for correction is also given in order to obtain two-dimensional flow characteristics. Also given are the equations for the evaluation of the pressure distribution measurements. Another contribution is made regarding the presentation of the test results in form of non-dimensional quantities.

Finally some of the results of systematic measurements of cascades with symmetrical aerofoil sections NACA 0010 are reported, and the above suggested method is applied for the evaluation of the measurements.

I. INTRODUCTION

The development of fluid flow machines has progressed over the last ten years, primarily using empirical methods. It was primarily

*From the Institute for Fluid Mechanics of the Braunschweig Institute of Technology (director H. Schlichting), Professor dissertation approved by the mechanical engineering department. (Prof. Dr. H. Schlichting and Prof. H. Blank, Prof. H. Petermann).

** Numbers in margin indicate pagination in foreign text.

due to the appearance of the gas turbine that it became clear that further increases in efficiencies of fluid flow machines depends very greatly on an in-depth knowledge of the flow-physical processes within the cascade, the basic element of fluid flow machines. Cascades in axial flow can be analyzed by rolling off a coaxial cylinder segment onto a plane, which reduces the problem to a two-dimensional problem, the problem of a plane cascade flow. This is why research on plane blade flow has become one of the most important foundations for the development of fluid flow machines. Many papers have treated the problem theoretically and experimentally. However, there has been no systematic investigation of the influence of individual geometric parameters of a blade configuration, either from the theoretical or the experimental point of view. /314

From the theoretical side, one can use boundary layer theory and simple methods for calculating potential flows through cascades, which leads to a systematic and rational analysis of the problem (see [16]). An experimental treatment of the problem has probably not been done because of the large number of parameters and the experimental difficulties. Often the results are only partially recorded, or not at all (see [17]). It seems that a large-scale experimental effort will not be possible because of the substantial effort involved. We believe that these problems can only be solved with a reasonable amount of effort, by using rational theoretical calculation methods to conduct systematic research on plane blade flow. In order to verify the theoretical calculations, enough experimental results must be used.

The Institute for Fluid Mechanics of the Braunschweig Institute of Technology, under the direction of Prof. H. Schlichting, for several years has attempted to contribute to a solution of the problem of blade cascade flow (see [19], [20]).

The present paper gives a summary on the problems of experimentation, and their solution. We also give a few results of systematic blade cascade measurements.

2. EXPERIMENTAL TECHNIQUE

2.1 General Design Characteristics of Cascade Test Stands

Even though the development of test stands for investigating cascade flows is over two decades old, it has not reached the state of

investigations of single wings. The reason for this is not only the importance of wings in aviation. The difficulties in the experimental technique and the required effort are considerably greater for a cascade than for a single profile. It is well-known that to achieve plane flow over a single profile, considerable effort is required, which involves careful sucking-away of the boundary layers which form at the end discs of the wing. In the case of a blade cascade, there should be flow deflection, and therefore a pressure jump in the cascade. It can only be maintained by separating the incoming and outgoing flow sides of a blade cascade, using fixed walls. This means that the blade cascade must be placed between two side walls, which impair the achievement of plane flow.

The following table gives a summary of several cascade test stands for incompressible flow. We also show the cascade test stand of the Braunschweig Institute of Technology. For small Mach numbers, the incompressibility of the flowing medium can be assumed, but this is not true in practice in general. Nevertheless, investigations in the incompressible range give a great deal of information about the flow behavior of the compressible flow, as long as the local overvelocities on the profile are less than the speed of sound, and therefore no compression shocks occur.

Except for special test facilities, and because of the strong changes in direction of the jets impinging on the cascade, in cascade test stands it is usually not possible to recover part of the flow energy by using a closed circuit, for the air. This is done in normal wind tunnels today. Because of this, and because of the relatively high flow losses produced by the blade cascade itself, the power requirements for cascade wind tunnels is in general greater than for normal wind tunnels with the same velocity. According to the way in which the air is directed, we can distinguish between pressure operation and suction operation in cascade test stands (Figure 1). In the case of pressure operation, the air is pressed into a closed incident channel by a blower, which supplies air to the blade cascade from a certain incident flow direction. In the case of suction operation, the air is sucked in from the outside. It passes through the blade cascade and is then directed to a blower. In the first case, free expulsion of the air is possible behind the blade cascade, which

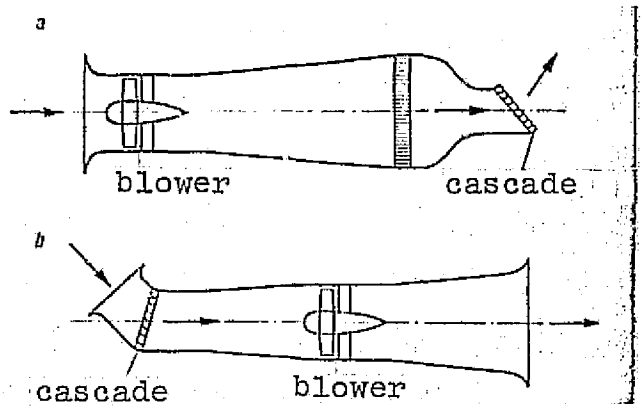

Figure 1: Designs of wind tunnels for cascade investigations
a) pressure operation b) suction operation

means that the outgoing flow direction, not known to begin with, cannot be disturbed by limiting walls having the wrong inclination. On the other hand, during suction operation, the sucked-in air is supplied to the blower behind the cascade in a closed channel, which means that the outflowing flow direction can be falsified. The sucked-in air can be allowed to flow into an underpressure chamber from which the air is again sucked away. The advantage of suction operation is the small wall boundary layer at the blade cascade inlet, if the suction cone is very short. Also, the drive power is reduced because of the reduced expulsion loss. Basically, pressurized operation with free outflow behind the cascade should be the most favorable configuration, and the present collection of references demonstrates this. However, for in- /315
termittent channels, in which operation occurs by letting air flow into a vacuum chamber, only suction operation is possible.

The Reynolds numbers used are in the range between 2×10^5 to 6×10^5. An increase in the Reynolds number up to 10^6 seems desirable, because most flow machines operate at these values, and even higher. This requires relatively large blade chords, which also increases the measurement accuracy. A blade chord of 200 mm should be a useful value.

Strictly speaking, a blade cascade is a row of infinitely many blade profiles arranged along a straight line, which can be approximated in experiments by a small number of blades. If the upper and lower limits (base walls) of the blade cascade are designed so that these walls are streamlines of the infinitely-long cascade, and if we avoid

Table 1: Design Characteristic of Several Plane Cascade Test Stands for Incompressible Flow

Reference	Author	Research Facility	Year of Publication	Type of Tunnel	Reynolds no.	Avg. no. of blade divisions	side ratio of blades	Boundary Layer Removal	Type of Measure-ment
1	K. Christiani	AVA Goettingen	1928	Pressure Operation free outflow	4×10^5	5	3	none	force, momentum, pressure distribution
2	C. Keller	E.T.H. Zurich	1934	Pressure Operation, free outflow	4×10^5	5	2.3	none	force, momentum, pressure distribution
3	H. Hausenblas	BMW Berlin	1951	Suction Operation, closed outflow	2×10^5	6	5	none	momentum, pressure distribution
4	W. T. Sawyer	E.T.H. Zurich	1949	Pressure Operation, closed outflow	2×10^5	8	3	slit suction at all walls	force, momentum, pressure distribution
5	F. G. Blight W. Howard H. McCallum	Aeronautic Research Lab Melbourne	1949	Pressure operation, free outflow	2×10^5	12	6	slit suction at all side walls	momentum, pressure distribution
6	A.D.S. Carter S. J. Andrews H. Shaw	Nat. Gas. Turb. Es-tablishm. Farnborough	1950	Pressure operation, free outflow	3×10^5	12	4	slit suction at floor walls	momentum, pressure distribution
7	C. Mortarino	Politechnikum Turin	1951	pressure operation, free outflow	4×10^5	6	3.5	none	momentum, pressure distribution

Table 1: (continued)

Reference	Author	Research Facility	Year of Publication	Type of Tunnel	Reynolds no.	Avg. no. of blade divisions	side ratio of blades	Boundary Layer Removal	Type of Measurement
8	J. R. Erwin J. C. Emery	N.A.S.A. Langley Field	1951	Pressure Operation, free outflow	4×10^5	6	4	slit suction at side walls, and wall suction within cascade	momentum, pressure distribution
-	N. Scholz	T.H. Braunschweig	1953	Pressure Operation free outflow	6×10^5	6	3	slit suction at all walls	momentum, pressure distribution

thick boundary layers at the base walls, then the flow can be considered to be a segment out of an infinite row of blades in a flow. The better we can match the boundary conditions, the smaller is the required number of blades, in order to obtain the flow of an infinte blade row in the central part of the blade cascade. Figure 2 shows several ways of designing the limiting walls for the blade cascade. Even though the streamlines deviate from parallel flow by about one blade chord in front of the cascade inlet, only a plane base wall can be used in practice. Immediately after this, we can have a flexible sheath at a distance of one-half a blade division from the last blade, which has approximately the shape of an average streamline. However, this requires a new shape for the sheath, for each cascade position. If the pressure differences in the cascade are not too large, it may be advantageous to use a free jet boundary along the final streamline. Another relatively simple solution consists of using a normal blade as the end wall, and the base wall is placed right up to the blade nose, approximately at the stagnation point of the blade in free flow. However, then the boundary /316
layer of the base wall impinges on the end blade, and this leads to a premature separation, so that it is advantageous to remove the boundary layer ahead of the cascade. One good solution to the problem may be to allow the base wall to terminate somewhat above the last normal blade,

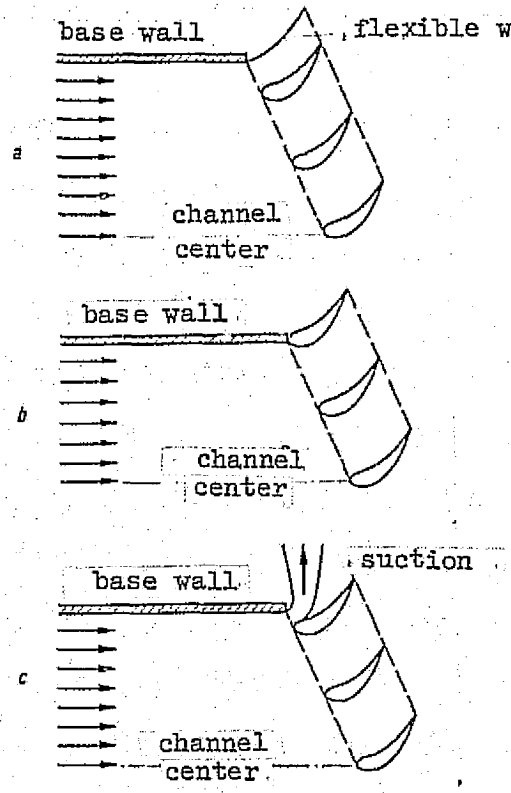

Figure 2: Designs of the end boundaries for measurements with plane cascades.

a) flexible end boundaries for one-half blade division
b) blade profile as end boundaries over an entire blade division
c) blade profile as an end boundary with suction.

and the intermediate air current is removed in a suction line. By regulating the amount sucked off, it is possible to displace the stagnation point at the final blade in such a way that the boundary conditions for the flow are satisfied. In order to regulate the suction amount, it is advantageous to install a static pressure tap at the base wall at some distance ahead of the grid cascade inlet. It must have the same static pressure as in the center of the channel. Even if there is a very large inclination of the cascade front, one can bring about a sufficiently constant static pressure variation along the cascade inlet, which otherwise leads to difficulties in many cases. Usually, it is not advantageous to expand the final wall behind the cascade beyond the cascade width, because the outflow direction is unknown. This would mean that the fixed walls would produce a change in the outflow direction. Because of the free jet boundary, the edge streamline is given a constant pressure. In general, the trailing edge pressure of

a cascade profile deviates only slightly from the pressure behind a cascade, so that a constant pressure along the boundary streamline satisfies the required boundary conditions with sufficient accuracy. However, in many cases, especially for highly-loaded turbine cascades, the pressure along the streamline which goes from the blade trailing edge changes so much that it is advantageous to dispense with the free jet boundary, and to use a plane fixed wall. Its inclination is best determined from the condition of constant static pressure along a plane parallel to the cascade.

One additional important problem are the measures for bringing about a plane flow in the central cross-section of the blades. Because of the boundary layers which are produced along the side walls, the flow is accelerated in the central part of the channel, so that downstream the flow increases in the central part of the channel cross-section. This jet contraction increases, the greater the boundary layer thickness is compared with the channel width and therefore with the blade height. There will be an especially great increase in the boundary layer growth at the side walls, within the blade cascade, because due to the interference between the blade boundary layer and the wall boundary layer and because of the pressure increase which especially occurs in the case of pumping cascades, the conditions which are produced along the blade contour are so unfavorable that dead water regions are produced in many cases there. This is true, even though there is healthy flow in the central part of the blade. The constriction of the cross-section at the cascade outlet determines the contraction of the flow in the central cross-section. This can have an effect upstream a large distance ahead of the blade cascade. Therefore, in many cases it is not sufficient to remove the boundary layer at the side walls around the cascade inlet alone, especially if a new wall boundary layer is produced inside the cascade with a substantial thickness. We can distinguish two types of boundary layer suction, and there can be intermediate kinds as well (Figure 3). One type, called "slit suction" is characterized by the fact that suction is done in the direction of the incoming flow. In the case of wall suction, the suction is perpendicular to the wall and therefore perpendicular to the main flow direction. In the case of the slit suction, a region corresponding to the boundary layer thickness of the flow is cut off, and is separated from the main

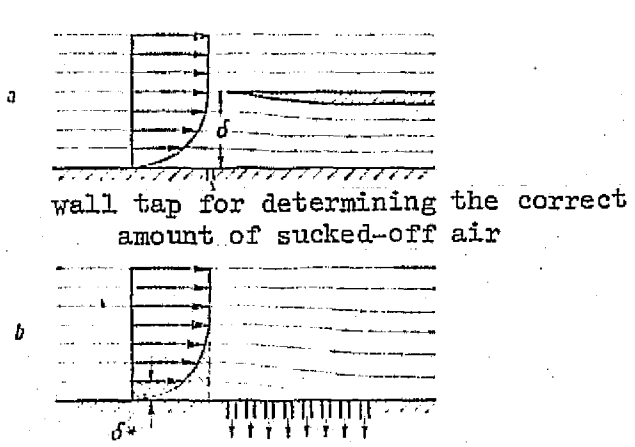

Figure 3: Designs of Boundary Layer Suction.
a) slit suction b) wall suction

flow which results in a reduction in the free channel cross-section. The wall suction method does not change the free cross-section but only so much air may be removed as corresponds to the displacement thickness of the boundary layer. In this case, the undisturbed out flow will /317 have again the original flow cross-section available, and any previous boundary layer disturbance will be restricted to the wall area if the channel width is large enough. The advantage of wall suction is the small amount which has to be sucked away, and the fact that the channel cross-section remains the same. However, the boundary layer removal is not as good as for slit suction. In addition, slit suction allows a much simpler adjustment of the suction amount. It can be adjustd so that the static pressure measured in a wall tap compared with the end of the slot becomes equal to the undisturbed static pressure in the center of the channel. This adjustment has been found to be very sensitive. The design of the slit suction device is much more difficult and was therefore only used to remove the boundary layer ahead of a break cascade. For the first time, J. R. Erwin and J. C. Emery [8] removed the boundary layer within the cascade using a wall suction method, and they were quite successful. The required suction power levels are quite substantial in every case, because there are substantial losses in the suction lines. We should also mention that when there is a pressure drop in the cascade, there is a possibility that the boundary layer can be removed without suction blowers using an overpressure which prevails ahead of the cascade.

2.2 Measurement Technique and Measurement Instruments

For the force measurement and the momentum measurement used for cascade measurements, the latter is simpler and more reliable, so that it is used almost exclusively in more recent investigations. The only advantage of a force measurement is that it is possible to determine the blade force of a blade, or of a blade segment, by weighing. Also, the measurement process is much shorter and can be more rapidly evaluated. In the momentum method, the flow is measured along one blade division behind the cascade at a series of points (wake measurement). This is a substantially more accurate method, and one can measure the local distribution of momentum along the blade height. In the force measurement technique, there is a substantial difficulty associated with the suspension of the measurement blade, which does not exist in the momentum measurement method. It is advantageous to perform pressure distribution measurements along the blade contour, to get a better insight into the flow processes within the blade cascade. The techniques used for this are the same as in any other pressure distribution measurements.

In the momentum measurement method, which is based on the momentum theorem between two planes parallel to the cascade ahead of and behind the blade cascade, it is necessary to measure the following three quantities in the incompressible case:

- 1) static pressure
- 2) velocity magnitude
- 3) velocity direction

at least along the blade division, ahead of and behind the cascade. Ahead of the cascade, at least in the region around the center of the channel, the three flow parameters are sufficiently constant. Therefore it is sufficient to measure these quantities at a suitable point ahead of the blade cascade, at a distance of about one blade chord. In general, it is not necessary to measure the flow direction ahead of the cascade, because this is the direction of the axis of the incident flow channel, which is appropriately regulated to be horizontal. Behind the cascade, the measurements are performed at several points within sufficiently small intervals along the blade central cross section in a plane parallel to the cascade. A probe holder which can be displaced parallel to the cascade is required for this. The distance

between the downstream measurement plane from the trailing edge plane of the blade cascade should be selected so that the static pressure along one blade division is approximately constant. The loss flow interval between the blades should have a region with no losses. In general, this is satisfied by distances between 10 and 50% of the blade chord behind the cascade, depending on the outflow angle.

There are three measurement variables, one for the front measurement plane "1" and two for the rear measurement plane* "2y". One of these, the static pressure, does not require an absolute measurement, but instead it is sufficient to know the pressure difference between two planes. This means that a total of five quantities must be measured. If we only consider differential pressures between the points within the flow as measurement variables, then we find that the following variables are suitable:

1. Stagnation pressure of incident flow, q_1
2. Static pressure difference, $p_2(y) - p_1$
3. Total pressure loss, $g_1 - g_2(y)$
4. Incident flow angle β_1
5. Outflow angle, $\beta_2(y)$

If we restrict the measurement to one blade division which is usually sufficient in most cases, then the measurement range of the plane "2y" parallel to the grid is adjusted so that the loss valley of the central blade will lie in the center of the measurement range. The measurement points inside the loss valley are located much more closely inside the loss valley because of the strong dependence of the measurement variables on y, than in the remaining region on both sides of the valley. One can have a very convenient method of calculating the required average measured values along one division, by using an even number of equidistant intervals between the individual measurement points, inside and outside the wake valley. The integration of the measurement variables is done by using the Simpson rule, and this is applied to each partial region using the equidistant

*The index y states that this is a plane, in which the measurement quantities still depend on the y coordinate (Figure 7).

intervals*.

In order to measure the static pressure, total pressure, and outflow angle in the wake at each point, it is appropriate to use combined measurement probes, which will simultaneously measure these three quantities at the same position. Figure 4 gives two designs of such probes. The design difficulty here is to measure the static pressure directly, without a calibration factor. We can accept the fact that the static

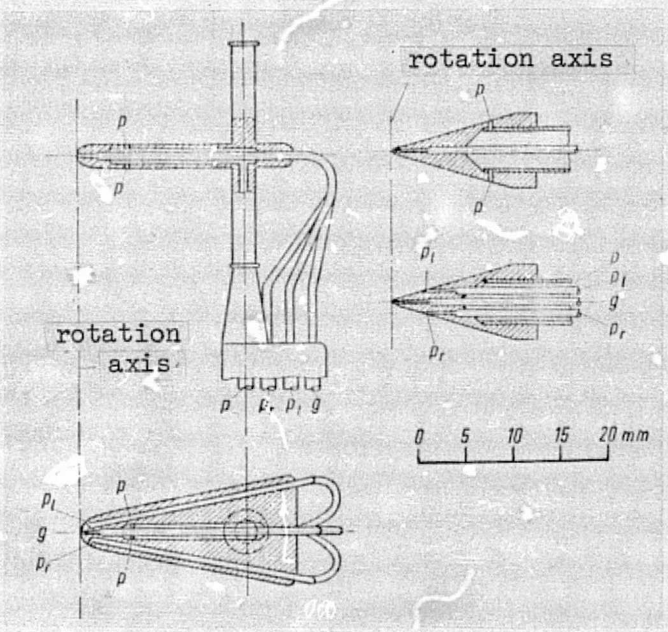

Figure 4: Designs of measurement probes for wake measurements behind plane cascades.

g = total pressure p = static pressure $p_r - p_l$ = flow angle.

pressure tap will usually be located at some distance downstream from /318 the total pressure tap, because the static pressure gradient is very small in the flow direction. The circular cylinder holders on the side are used to correct the static pressure of the left probe. Depending on the diameter, this results in a stagnation at the static pressure

---

*If M is the average value of a measurement variable f, then it is given by a sum formula $M = \Sigma f_n g_n / \Sigma g_n$. Then the wakes g_n will take on the following values, if h is the measurement point interval outside of the wake valley and i is the (smaller) measurement point interval inside the wake valley. For measurement points outside of the valley:

For measurement points outside of the valley, g_n = h, 4h, 2h, ..., 4h

For measurement points at the edge of the valley, g_n = h + i

For measurement points inside the valley, g_n = 4i, 2i, 4i, ... 4i.

taps located in front of this point. This equalizes the overvelocity by the displacement of the probe head. In the right probe, the static pressure can be corrected by removing the conical, or cylindrical, part of the probe head. The symmetrically arranged taps used for angle measurement, can lead to erroneous measurements if the flow is highly inhomogeneous, if the taps are too far apart. However, usually the errors are within the measurement accuracy. Directional sensitivity of the probes is only required perpendicular to the main flow plane, because the probe is adjusted parallel to the flow using the zero method, then measurements are performed.

2.3 The Cascade Test Stand of the Braunschweig Institute of Technology, Fluid Mechanics Department.

In the design of the cascade test stand to be described below, we were concerned with the points discussed above as well as the possibility of carrying out systematic cascade measurements for all cascade configurations which occur in practice.* We are especially concerned with reducing the conversion time between measurements for two cascade configurations. The three most important parameters of plane cascade configurations:

- 1) Division ratio t/l
- 2) Blade angle, β_S
- 3) Incident angle, β_1

should be continuously measureable over ranges which occur in practice, and with a small amount of effort. By achieving a perfect flow at the terminal members of the cascade, we wanted to keep the blade number as small as possible, in order to reduce the production effort for each special blade shape as much as possible. Finally, we wish to bring about a plane flow in the center of the channel cross-section, in order to have perfect comparisons with theoretical calculations of plane blade cascades.

Figure 5 gives a schematic representation of the test stand. The wind tunnel of the Fluid Mechanics Institute of the Braunschweig Institute of Technology was available for operating the test stand, with a free jet nozzle having a diameter of 1.3 m. Following this,

*Engineer H. Goldmann contributed substantially to the design.

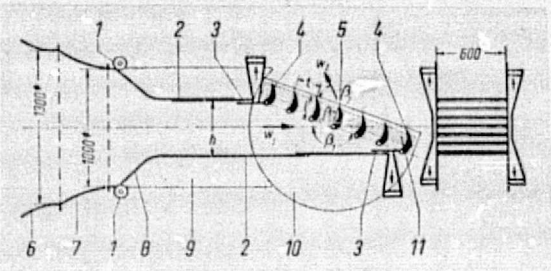

Figure 5: Sketch of a plane cascade test stand at the Institute for Fluid Mechanics of the Braunschweig Institute of Technology.

1- tension roller
2- sides of the incident flow channel
3- suction slit
4- end blade
5- measurement blade with pressure caps
6- wind tunnel nozzle
7- reduction nozzle
8- inlet nozzle
9- side wall
10- rotating disc
11- wall suction

(The height h of the incident flow angle can be adjusted between 300 and 800 mm).

there is a reduction nozzle, which reduces the flow cross-section to a 1 x 0.6 m rectangle. After this, the test stand proper follows, with parallel side walls and floors which can be varied in height by spindles. Together, they make up the flow channel. Because of the changeable height of the incident flow channel, an inlet nozzle to the incident flow channel is made up of two flexible sheets which come after the base sheets and which are stretched to the required length by means of stretching rollers. The side walls are continued by two semicircle discs, which can be rotated around a horizontal axis at the height of the center of the channel (change in β_1) and which are rigidly connected. The blades of the cascade, which are normally 200 mm deep and 600 mm wide, are placed between these walls. They are attached so that they can be rotated around the center of the profile nose radius (change in β_S) and they can also be displaced parallel along the cascade front (changeability of t/l). The end surfaces of the cascade are made as normal blade profiles, and the bases of the incident flow channels can also be rotated around the center of the profile radius. The bases consist of two sheets which can slide inside one another, so that their length can be changed depending on cascade position.

The boundary layer removal is done using a slit suction device /319 and occurs 200 mm ahead of the terminal blades along the base walls, and the slit suction is 30 mm high. The wall suction is located along the side walls, along a 100-mm wide strip within the blade cascade width. For velocities up to 50 m/s inside the rectangle cross-section, it is possible to remove up to 10% of the amount flowing through by suction. The suction power is 2 m^3/s with a pressure of 500 mm water column. Figure 6 shows the test stand.

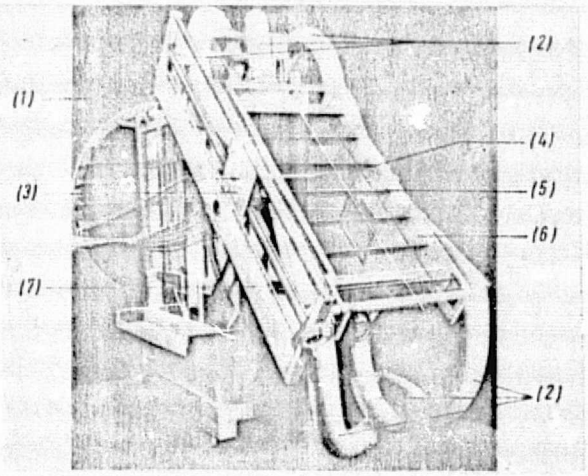

Figure 6: View of a Plane Cascade Test Stand at the Institute for Fluid Mechanics of the Braunschweig Institute of Technology.

3. EVALUATION OF CASCADE EXPERIMENTS

3.1 Determination of the Outflow and the Blade Forces from Wake Measurements*.

The use of the momentum method for determining the flow resistance of a single airfoils and blade cascades has been found to be very reliable for a long time. In addition, when this method is used for blade cascades, and by also measuring the flow angle, one also obtains the lift of the blade. This means that it is the method suited for investigating the blade cascade flows. It is remarkable that no theoretical foundations for the use of the momentum method have been formulated for blade cascade flows. However, the corresponding evaluation formulas have been used and developed, that is, the Betz or the Jones formulas. In very many wake measurements of blade cascades, one only

*The author [22] already reported on this.

forms the average value of the measured values over one blade division. However, these average values depend on the distance between the measurement plane and the blade cascade, and compared with the homogeneous translation flow, which would occur at a large distance behind the blade cascade, there can be errors on the order of up to 20%, which not only occur in the flow loss value, but also in the static pressure and the outflow angle. It is not important whether a second blade cascade is to be arranged at a small distance behind the blade cascade, because the homogeneous incident flow for the second cascade can only be a homogeneous translation flow, and it must be equivalent to the inhomogenous flow in the measurement plane in terms of momentum and energy.

In order to determine the flow variables of the homogeneous flow, we will formulate the momentum theorem on a control surface, K_1 (Figure 7), which is located between two streamlines at a distance of one blade

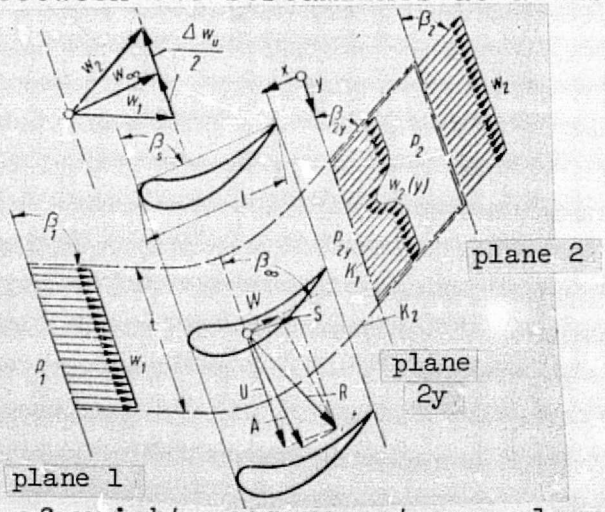

Figure 7: Evaluation of weight measurements on plane cascades.

division from the measurement plane "2y" from the plane "2" as far back behind the cascade where the homogeneous flow condition is satisfied. Then the continuity equation gives

$$\varrho\, w_2 \sin\beta_2 = \varrho\, \frac{1}{t}\int_y^{y+t} w_{2y}(y)\sin\beta_{2y}(y)\,dy, \tag{1}$$

and the momentum theorem perpendicular to the cascade front gives

$$\left\{\begin{array}{l} p_2 + \varrho\, w_2^2 \sin^2\beta_2 = \\ \quad = \dfrac{1}{t}\displaystyle\int_y^{y+t} p_{2y}(y)\,dy + \varrho\,\frac{1}{t}\int_y^{y+t} w_{2y}^2(y)\sin^2\beta_{2y}(y)\,dy, \end{array}\right. \tag{2}$$

and the momentum theorem parallel to the cascade front gives

$$\left\{\begin{array}{l} \varrho \sin\beta_2\cos\beta_2\, w_2^2 = \\ \quad = \varrho\,\dfrac{1}{t}\displaystyle\int_y^{y+t} w_{2y}^2(y)\sin\beta_{2y}(y)\cos\beta_{2y}(y)\,dy. \end{array}\right. \tag{3}$$

In the last equation, one should also, strictly speaking, consider the shear stresses in the plane "2y", but they are negligible in practice, which has been discussed by W. Traupel [9]. Using equations (1) - (3), we can determine the velocity w_2, the static pressure p_2, and the outflow angle β_2 of the homogeneous flow from the measured quantities from the plane "2y". However, we will introduce the simplification here that with substantially facilitate the evaluation. It is natural to substitute a constant value for the angle distribution in the plane "2y", because in momentum measurements of single air foils, the local flow angles is not considered, which does not lead to any substantial errors. With this simplification, we ob- /320
tain the following values for the homogeneous flow behind the cascade from the three equations given above, if β_{2y} is the constant average of the outflow angle in the plane "2y"*.

$$w_2^2 = w_{2u}^2 + w_{2m}^2 = \sin^2\beta_{2y}\left(\frac{1}{t}\int_y^{y+t} w_2(y)\,dy\right)^2 + \cos^2\beta_{2y}\left[\frac{1}{t}\int_y^{y+t} w_2^2(y)\,dy\right]^2 \cdot \left[\frac{1}{t}\int_y^{y+t} w_2(y)\,dy\right]^2 \tag{4}$$

$$p_2 = \frac{1}{t}\int_y^{y+t} p_2(y)\,dy + \varrho\sin^2\beta_{2y}\left[\frac{1}{t}\int_y^{y+t} w_2^2(y)\,dy - \left(\frac{1}{t}\int_y^{y+t} w_2(y)\,dy\right)^2\right], \tag{5}$$

$$\operatorname{ctg}\beta_2 = \operatorname{ctg}\beta_{2y}\,\frac{\frac{1}{t}\int_y^{y+t} w_2^2(y)\,dy}{\left(\frac{1}{t}\int_y^{y+t} w^2(y)\,dy\right)^2}. \tag{6}$$

*If we consider the variability of β_{2y} with y, then we obtain formulas given in the appendix.

In order to obtain formulas for the practical evaluation, we will introduce the following dimensionless variables:

The nondimensional total average pressure loss

$$G = \frac{1}{t}\int_{y}^{y+t} \frac{g_1 - g_2(y)}{q_1}\, dy, \tag{7}$$

The nondimensional average pressure difference

$$P = \frac{1}{t}\int_{y}^{y+t} \frac{p_2(y) - p_1}{q_1}\, dy, \tag{8}$$

The correction term

$$K = \frac{1}{t}\int_{y}^{y+t} \frac{q_2(y)}{q_1}\, dy - \left(\frac{1}{t}\int_{y}^{y+t} \sqrt{\frac{q_2(y)}{q_1}}\, dy\right)^2. \tag{9}$$

Since the linear average is always greater than the average squared of a square root, K is a correction term which is always greater than 0 and is also small compared with the integral values of the right side of equation (9). If we substitute this quantity in (4), (5), and (6), then after a calculation (see Appendix B) we obtain the following formulas for converting average values of inhomogeneous flow to an equivalent homogeneous flow:

$$\frac{\Delta g}{q_1} = \frac{g_1 - g_2}{q_1} = G - K, \tag{10}$$

$$\frac{\Delta p}{q_1} = \frac{p_2 - p_1}{q_1} = P + 2K\sin^2\beta_{2y}, \tag{11}$$

$$\frac{q_2}{q_1} = 1 - P - G + K(\cos^2\beta_{2y} - \sin^2\beta_{2y}), \tag{12}$$

$$\operatorname{ctg}\beta_2 = \left(1 + \frac{K}{1 - P - G}\right)\operatorname{ctg}\beta_{2y}. \tag{13}$$

The angle β_{2y} is a suitable average value of the flow angle in the plane "2y". Since the angle differences are always small, the method of averaging is not important. One suitable averaging method consists of averaging using the cotangent of the angle, because essentially this is an averaging over the velocity components parallel to the grid front. The formulas given above show that in a blade cascade flow not only the total pressure loss, but also the static pressure and

the outflow direction differs from the equivalent homogeneous flow, compared with the average value of the inhomogeneous flow*.

In order to use the formulas (10) - (13), we require the average values of the total pressure, static pressure, and outflow angle in the measurement plane "2y", as well as the correction quantity K given by equation (9). It is rather difficult to calculate. However, since it is a correction quantity, it is natural to calculate it once and for all for approximating the weight valley using an analytical function, as was already done by C. Keller [2] for the special case $\beta_2 = 90°$ using a cosine function. For momentum measurements on a single profile, this was done by A.D. Young [10], and he obtained exceptional agreement with the results of a normal evaluation. One condition for calculating a universal correction quantity for cascade weight measurements is that the individual wake values will not empty into one another, and that also the static pressure along a blade division is sufficiently constant, so that between the weight values there will be a region with contant velocity. In practical cases, these conditions are always met with sufficient accuracy.

We will use the Gauss air-distribution function for approxiating the velocity valley in the wake, which follows from the theoretical analysis of the distribution of a plane turbulent wake some distance behind the body (see for example, H. Schlichting: Boundary Layer Theory, G. Braun, Karlsruhe, 1951, p. 447). We will set (see Figure 8)

$$w_{2\max} - w_2(\eta) = (w_{2\max} - w_{2\min})\, e^{-c^2\eta^2}. \tag{14}$$

Here, w_{2max} is the velocity outside of the velocity valley and /321 w_{2min} is the smallest velocity inside the valley, and η is the dimensionless coordinate y/t. The zero of the y-axis is selected so that $w_2(\eta) = w_{2min}$ for $\eta = 0$. Therefore, the value is symmetric with respect to the origin. If the static pressure is constant inside the valley, then

*W. T. Sawyer [4], derived a formula for the pressure p_2, by assuming the same outflow angles in the planes "2y" and "2" and the momentum theorem is formulated in outflow directions. In our notation, he obtains $(p_2 - p_1)/q_1 = P + 2K$. However, this result is not compatible with the momentum theorem perpendicular to the outflow direction. The results are only identical in the special case $\beta_2 = 90°$, which was treated by C. Keller [2].

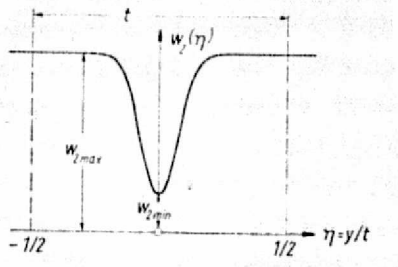

Figure 8: Turbulent wake profile according to Equation (14).

the loss valley of the total pressure $g_2(y)$ is identical with the stagnation pressure valley $q_2(y)$. We therefore can relate the maximum total pressure loss $g_1 - g_{2min}$ to the velocity difference $w_{2max} - w_{2min}$. We will introduce the following dimensionless parameters:

$$a = \frac{w_{2min}^2}{w_{2max}^2} = 1 - \frac{1}{1-P}\,\frac{g_1 - g_{2min}}{q_1} \tag{15}$$

P is the average of the static pressure, according to (8). The free parameter c of equation (14) can be related to the total content of the velocity valley, and therefore the content of the total pressure loss valley, which is given by the average of the total pressure loss G in equation (7). The integration of the wake valley over η, which, strictly speaking, runs over 1 blade division from $\eta = -1/2$ to $\eta = +1/2$, can be extended to infinity without any problem, because the error distribution function (14) decays very rapidly towards the outside. Therefore, after a few calculations we obtain the following for the parameter c (see appendix C):

$$c = \left[2\sqrt{\pi}\,(1-\sqrt{a}) - \sqrt{\frac{\pi}{2}}\,(1-\sqrt{a})^2\right]\frac{1-P}{G}. \tag{16}$$

Now the correction term K of equation (9) can be universally calculated by introducing the trial solution equation (14) for the velocity distribution, and this can be related to the average total pressure loss G. One then obtains (see Appendix C):

$$\frac{K}{G} = \frac{(1-\sqrt{a}) - \frac{2}{2\sqrt{2}-(1-\sqrt{a})}\,\frac{G}{1-P}}{2\sqrt{2}-(1-\sqrt{a})}. \tag{17}$$

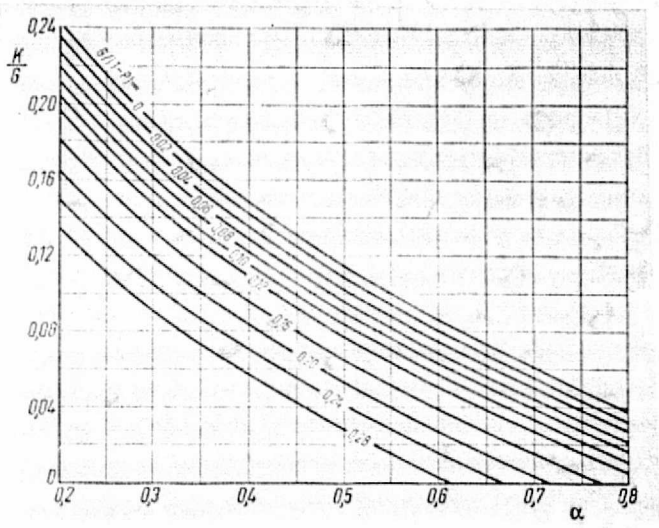

Figure 9: Universal calculated correction member according to Equation (17).

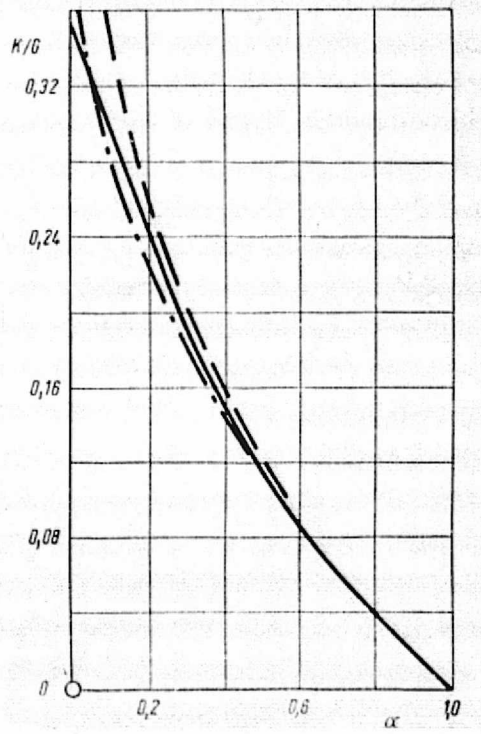

Figure 10: Comparison of universally calculated correction terms for the special case of a single profile.

This function is shown in Figure 9 and Table 2 as a function of the parameter α and G/(1 - P). In addition, to the quantities G and P required for the evaluation, we must determine the value of α according to equation (15) from the wake measurement, in order to determine the

Table 2: Universal Correction Terms K/G according to equation (17).

$\frac{G}{1-P}$ / α	0	0,02	0,04	0,06	0,08	0,10	0,12	0,16	0,20	0,24	0,28
0,2	0,2431	0,2353	0,2276	0,2199	0,2122	0,2044	0,1967	0,1812	0,1648	0,1503	0,1349
0,3	0,1902	0,1832	0,1761	0,1690	0,1619	0,1548	0,1477	0,1335	0,1200	0,1057	0,0914
0,4	0,1491	0,1425	0,1359	0,1293	0,1227	0,1161	0,1095	0,0963	0,0829	0,0699	0,0565
0,5	0,1156	0,1093	0,1031	0,0969	0,0907	0,0845	0,0782	0,0658	0,0532	0,0410	0,0284
0,6	0,0869	0,0809	0,0751	0,0691	0,0632	0,0573	0,0514	0,0396	0,0273	0,0157	0,0038
0,7	0,0616	0,0559	0,0503	0,0447	0,0390	0,0334	0,0277	0,0165	0,0049	--	--
0,8	0,0389	0,0335	0,0281	0,0227	0,0173	0,0119	0,0065	--	--	--	--

correction K. The fact that equation (1) can also give values of $K < 0$ is due to the fact that in these cases, we have wake values which already transfer into one another and for these, the present theory is no longer valid.

Comparison of the correction term recalculated and the theory of C. Keller [2] and A. D. Young [10], which is only possible for the case $G/(1 - P) = 0 (t/l \to \infty)$ is shown in Figure 10. We only find substantial differences for very small α (very steep valley profile), /322 and the cosine form of the valley by the other authors is too full compared with the error distribution function. Comparison calculations with wake measurements of the author on plane blade cascades show very good agreement between the universally-calculated correction term of (17) and the numerically-calculated correction term using equation (9). Also, we cannot find any deviation compared with evaluation results which were performed using a distribution of the outflow angle in the wake which varies with y, within the calculation accuracy (see Table 3).

It is possible to determine the blade forces in the simple way from the homogeneous translation flow calculated for the plane "2". For this purpose, we will consider a control surface K_2 (Figure 7), which extends from the plane "1" ahead of the cascade to the plane "2" behind the cascade between two congruent streamlines at a distance of one blade division. For this surface, the momentum theorem in the x and y direction and the plane continuity equation, are given by:

$$U = \varrho t (w_2^2 \sin\beta_2 \cos\beta_2 - w_1 \sin\beta_1 \cos\beta_1), \tag{18}$$

$$S = \varrho t (w_2^2 \sin^2 \beta_2 - w_1^2 \sin^2 \beta_1) + t (p_2 - p_1), \tag{19}$$

$$w_1 \sin \beta_1 = w_2 \sin \beta_2. \qquad * \tag{20}$$

From this, we find the following values for the dimensionless coefficients of the circumferential force U parallel to the cascade front and the shear force S perpendicular to the cascade front

$$c_U = \frac{U}{\varrho w_\infty^2 l/2} = 2 \frac{t}{l} (\operatorname{ctg} \beta_2 - \operatorname{ctg} \beta_1) \sin^2 \beta_\infty, \tag{21}$$

$$c_S = \frac{S}{\varrho w_\infty^2 l/2} = \frac{t}{l} \frac{p_2 - p_1}{q_1} \sin^2 \beta_\infty, \tag{22}$$

where the reference velocity w_∞, which makes the angle β_∞ with the cascade front, is the vector average of w_1 and w_2. The angle β_∞ is found from

$$\operatorname{ctg} \beta_\infty = \frac{1}{2} (\operatorname{ctg} \beta_1 + \operatorname{ctg} \beta_2). \tag{23}$$

A recalculation to dimensionless coefficients for lift A perpendicular to w_∞ and drag W parallel to w_∞ gives:

$$\left\{ \begin{aligned} c_A &= c_U \sin \beta_\infty - c_S \cos \beta_\infty = \\ &= 2 \frac{t}{l} \sin \beta_\infty (\operatorname{ctg} \beta_2 - \operatorname{ctg} \beta_1) + \\ &\quad \frac{t}{l} \frac{\sin^2 \beta_\infty \cos \beta_\infty}{\sin^2 \beta_1} \frac{\lambda_g}{q_1}, \end{aligned} \right. \tag{24}$$

$$c_W = -c_S \sin \beta_\infty - c_U \cos \beta_\infty = \frac{t}{l} \frac{\sin^3 \beta_\infty}{\sin^2 \beta_1} \frac{\lambda_g}{q_1} \tag{25}$$

It is remarkable that the formula for lift contains the friction loss in the second term. As shown in [16], this quantity is an additional list which is produced by the pressure loss in the cascade, and has

---

*Here and in the following we will use the following sign conventions, for angles and forces: the zero-direction for β is the cascade front in the section side - pressure side direction of a blade, a positive rotation direction is clockwise. Then we have U > 0 for the forces, $\beta_1 > \beta_2$, S > 0, $p_1 < p_2$, A > 0, $\beta_1 > \beta_2$, W > 0 in the direction of w_∞.

the magnitude $A_F = W \operatorname{ctg} \beta_2$

3.2 Correction of the Influence of the Jet Contraction

In spite of various measures for removing the side wall boundary layers, it is not always possible to completely avoid a contraction of the flow in the central cross-section of the channel. As long as this jet contraction is small and which results in an acceleration of the basic flow in the central cross-section, it is possible to ignore its influence on the boundary layer formulation at the contour of the blade profile. It then becomes possible to carry out a correction of the measurement results with respect to the jet contraction which occurs. The various contributions on this problem (see [7, 8, 12, 14]) only specify corrections without any reasons.

Because of the displacement effect of the side wall boundary layers, the incident flow tail is closed, the amount of flow through one blade division referred to the width "1"

$$Q(x) = \int_{y}^{y+t} w(x;y) \sin \beta(x;y)\, dy \tag{26}$$

increases in the central section of the channel from the value Q_1 in the measurement plane "1", to the value Q_2 in the measurement plane "2" (Figure 11). In order to simply calculate these relationships, we will assume that inside the cascade the flux has the magnitude Q_G and this occurs in the plane "G", whose position is determined by the lift center of gravity of the cascade profiles. This means that we have "concentrated" the blade cascade in the plane "G".

In order to satisfy the plane continuity equation between the measurement planes "1" and "2", it is necessary to increase the inlet velocity to the value

$$w_{1\,kor} = \frac{Q_G}{Q_1} w_1 = \mu_E w_1 \tag{27}$$

and reduce the outlet velocity to the value

$$w_{2\,kor} = \frac{Q_G}{Q_2} w_2 = \frac{1}{\mu_A} w_2 \tag{28}$$

We will define $\mu_E = Q_G/Q_1 > 1$, which is the inlet contraction coefficient, and $\mu_A = Q_2/Q_G$ is the outlet contraction coefficient*. Since the total pressure of the flow remains unchanged because of the jet contraction, accordingly, the pressures p_1 and p_2 must be corrected according to the velocity changes:

$$p_{1kor} = p_1 - (\mu_E^2 - 1) q_1, \tag{29}$$

$$p_{2kor} = p_2 + \left(1 - \frac{1}{\mu_A^2}\right) q_2. \tag{30}$$

We now must investigate the influence of the jet contraction on the outflow angle**. For this, we will apply the momentum theorem to the spatial control surface in the central cross-section of the flow (see Figures 11a and b). The upper and lower limiting surfaces of the control surfaces are two streamlines separated at a distance of one blade division. The side limiting surfaces are parallel planes, perpendicular to the cascade front plane with a very small distance Δz (Figure 11b). Upstream, the control surface is limited by the plane "G", where the blade cascade is considered to be concentrated as a series of vortices. Downstream, it is limited by the plane "2". In order to apply the momentum theorem, it is not necessary to know the flow distribution in the plane "G". It is sufficient to know the momentum which flows into the plane "G". But in the plane "G", the flow is given a momentum in the y-direction, such that the homogeneous flow behind the cascade is given the outflow angle β_{2kor} if there is no contraction between the planes "G" and "2", that is;

/323

$$I_G = \varrho Q_G w_{2kor} \cos \beta_{2kor}. \tag{31}$$

The momentum which occurs in the plane "2" with homogeneous flow is given by:

---

*One correction to the results of momentum measurements behind blade cascades regarding the jet contraction was also carried out by C. Mortarino [7]. The influence of the jet contraction on the outflow angle was not considered. If we do not assume any outlet contraction, ($\mu_A = 1$), then the correction given by Mortarino is identical with our correction formula.

**The information was already published in [18].

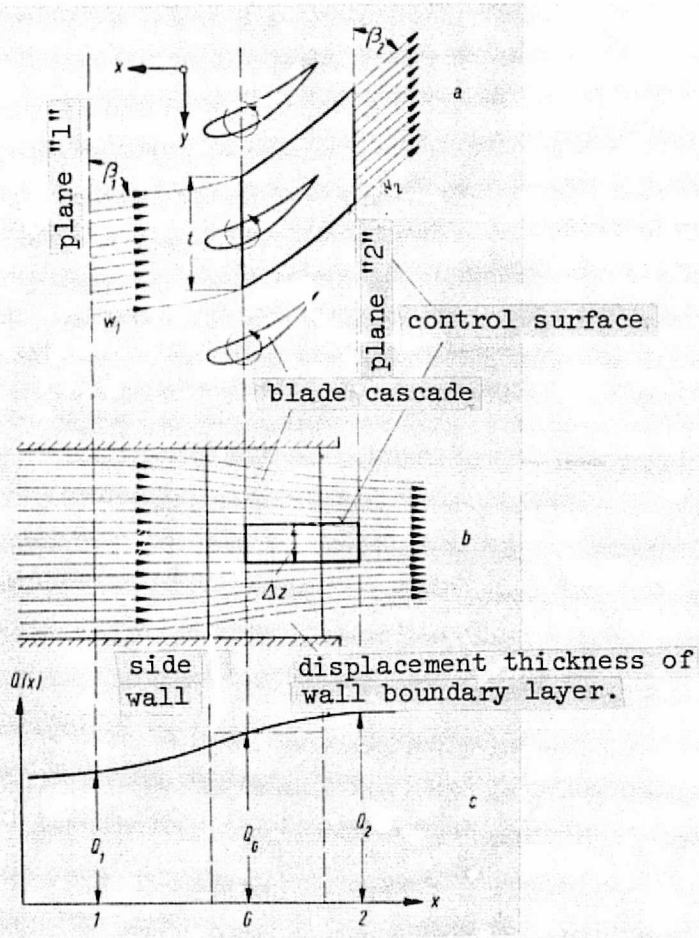

Figure 11: Calculation of an outflow angle correction due to jet contraction.

$$I_A = \varrho Q_2 w_2 \cos\beta_2. \tag{32}$$

Because of the contraction of the flow from the plane "G", towards the plane "2", there is an additional momentum which enters from the side limiting surfaces of the control surface. The amount flowing in is: $\Delta Q = Q_A - Q_E$, and the y-component of the velocity with which this amount flows into the control surface is not directly known. However, it must lie between the y-component in the plane "G" and the y-component in the plane "2", and therefore it is natural to use the arithmetic mean of these two components as the approximate value. This means that the additional incoming momentum is given by:

$$\Delta I = \varrho(Q_2 - Q_G)\tfrac{1}{2}(w_{2\,kor}\cos\beta_{2\,kor} + w_2\cos\beta_2). \tag{33}$$

Since there are no external forces which are applied to the control surface in the y-direction, the incoming and outgoing momenta must be equal: $I_E + I = I_A$. This gives the following equation for the corrected outflow angle (see Appendix B):

$$\operatorname{ctg}\beta_{2\mathrm{kor}} = \frac{Q_2}{Q_G}\operatorname{ctg}\beta_2 = \mu_A \operatorname{ctg}\beta_2 \tag{34}$$

This result states that the tangential components of the flow are not changed due to the contraction, but only the normal components are changed according to the increased amount of flow.

In order to apply the correction formulas derived above, we require the flows in planes "1", "G", and "2". In the plane "1", the flux is known from a measurement. Also, the flux in the plane "2" is known because the homogeneous flow in the plane "2" was determined from the measurement results in the "measurement plane 2y". On the other hand, the flux in the plane "G" is not directly known, and is difficult to measure. If we relate the increase in the fluxes from the "1" downstream, that is, the quantity $Q(x) - Q_1$, to the total increase in the flux between the planes "1" and "2", that is, $Q_2 - Q_1$, then we can expect that this function will be universal for a fixed position of the planes "1" and "2", independent of the total contraction. We will call this quantity

$$\kappa(x) = \frac{Q(x) - Q_1}{Q_2 - Q_1} \tag{35}$$

the contraction function. Let us assume it has been determined once and for all for a certain test stand, for example, by measuring the velocity along the channel center between planes "1" and "2y" without the installed blade cascade. We will achieve an arbitrary jet contraction by slightly reducing the outlet cross-section of the flow channel. Figure 12 shows this contraction function for the cascade test stand of the Fluid Mechanics Institute at the Braunschweig Institute of Technology, which was described above. Since we only have small values of the total contraction, it is not necessary to know /32
k(x) with any great accuracy, so that we can consider that the selection of the plane "G" in which the blade cascade is considered to be concentrated is not very important. The estimation of the center of lift of the blades is therefore sufficient for selecting a value of

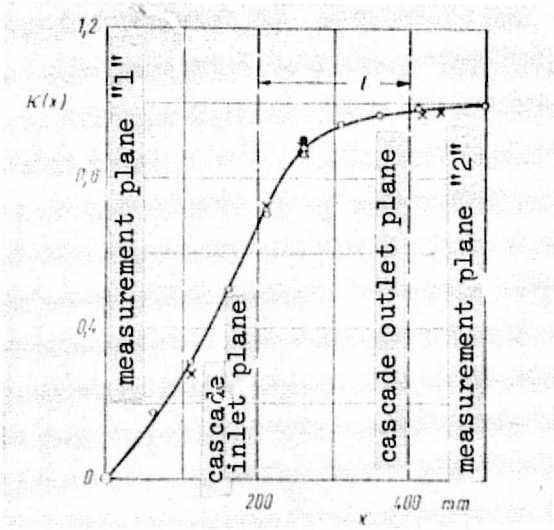

Figure 12: Universal contraction function for plane cascade test stand of the Braunschweig Institute of Technology, Fluid Dynamics Institute.

κ for a special cascade measurement. From the measurement, we obtain the total contraction coefficient μ_{ges} from

$$\mu_{ges} = \frac{Q_2}{Q_1} = \frac{w_2 \sin \beta_2}{w_1 \sin \beta_1} \tag{36}$$

After selecting a value for the contraction function $\kappa(x)$, according to the position of the lift center of gravity, we then find the inlet contraction coefficient

$$\mu_E = \frac{Q_G}{Q_1} = \kappa(\mu_{ges} - 1) + 1 \tag{37}$$

and therefore the outlet contraction coefficient

$$\mu_A = \frac{Q_2}{Q_G} = \frac{\mu_{ges}}{\mu_E} \tag{38}$$

In this connection, we have to consider another phenomena in the flow through a blade cascade with side wall boundary layers. Inside the curve blade channel, the particles with flow in the side wall boundary layers are subjected to a pressure gradient in the blade channel which is normal to the blade. Because of their reduced velocity, they cannot establish a dynamic equilibrium, which prevails outside of the boundary layer. Therefore, the migrating particles are pushed away in the

direction of the pressure gradient. A secondary flow results, as shown in Figure 13, for a plane parallel to the cascade behind the blade cascade. Discontinuity surfaces start at the blade trailing edges, just like a single air foil in a three-dimensional flow*, and inside the blade channels, secondary vortices are formed. Various authors [11, 12] believe that, due to the departing secondary vortices, that there is an induced downwind in the central cross-section of the flow channel, which changes the outflow direction of the plane blade cascade. However, it can easily be seen that the total circulation inside the dashed curves K must be 0. W. Traupel [13] gave an extensive explanation for this. It must be deduced that in the central section of the flow cross-section, the induction effect of this vortex system is cancelled, at least on an average, so that there is no influence on the outflow direction in the central cross-section. Of course, we assume that there is a sufficiently wide piece of undisturbed flow in the central part of the blade.

3.3 Evaluation of the Pressure Distribution Measurements

When measuring the pressure distribution along the blade contour, it is appropriate to select the quantities in the measurement plane "1", as reference variables. We must consider that because of the inlet contraction, they must be corrected according to equations [27) and (29). The dimensionless pressure distribution coefficient is then given by

$$c_p = \frac{p - p_{1\,kor}}{q_{1\,kor}} = \frac{1}{\mu_{\vec{I}}} \frac{p - p_1}{q_1} + 1 - \frac{1}{\mu_{\vec{E}}^2}. \qquad (39)$$

This correction can only be performed if the jet contraction is known from a wake measurement.

If we ignore the usually-small friction forces along the blade contour, then by integration of the pressure distribution along the blade contour, we can approximately determine the resulting blade force. Using a coordinate system normal (n) and tangential (t) to the blade chord, the dimensionless normal force is given by

*The physical reasons for these discontinuity surfaces are different, however; see [13].

$$c_{N1} = \frac{N}{q_1 l} = \oint_K c_p \, d\frac{t}{l} = \sum_\nu (g_\nu)_N c_p \qquad (40)$$

and the dimensionless tangential force is given by

$$c_{T1} = \frac{T}{q_1 l} = \oint_K c_p \, d\frac{n}{l} = \sum_\nu (g_\nu)_T c_p \qquad (41)^*$$

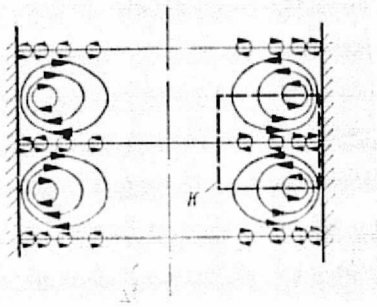

Figure 13: Influence of the vortex system for plane blade cascades on the outflow direction in the central section of the blades.

---

*We will give these coefficients the subscript 1, because in contrast to c_U, c_S, c_A, c_W they are referred to w_∞ and not w_1. For convenient numerical integration it is appropriate to replace the integrals by sums. The integration weights g_ν are determined from the distances from the individual measurement points parallel and perpendicular to the chord direction. These distances are not equidistant. If we assume a parabolic interpolation between three points each, according to the Simpson rule, for equidistant intervals, then we find according to E. Eltermann (ZAMM 33 (1953), p. 254), the following weights:

are even: $g_\nu = \frac{2}{3}h_\nu + \frac{2}{3}h_{\nu-1}$

are odd: $g_\nu = -\frac{1}{6}h_{\nu-1} + \frac{2}{3}h_\nu + \frac{2}{3}h_{\nu+1} - \frac{1}{6}h_{\nu+2}$

ν are the numbers of the measurement points on the profile contour which are numbered sequentially around the closed contour. $h_{\nu-1}$ is the distance between the measurement points $\nu-1$ and ν, $h_{\nu+1}$ is the distance between the measurement points ν and $\nu+1$ etc. Using the positive t and n directions (+t from the leading edge to the trailing edge, +n from the pressure side to the suction side of the blade profile), one must consider the sign of h_ν. We do not have to consider the position of the measurement point on the suction side and the pressure side. The beginning of the measurement point numbering has no influence (practically) on the sum results if there are sufficient measurement points, but an even number of measurement points is appropriate.

We can immediately recalculate these force components as circumferential forces and shear force or lift force and drag force. On the other hand we can determine the flow variables of the departing flow from these force components, by using the momentum theorem in the x and y directions. We again obtain equations (18) and (19), but now the forces U and S are known, and the equations are to be solved for the flow va- /325
riables. After a calculation, we obtain (see appendix E):

$$\frac{\Delta p}{q_1} = \frac{p_2 - p_1}{q_1} = -\frac{l}{t}\,(c_{N1}\cos\beta_s - c_{T1}\sin\beta_s), \tag{42}$$

$$\left\{\begin{aligned}\frac{q_2}{q_1} = 1 + \frac{l}{t}\,(c_{N1}\sin\beta_s - c_{T1}\cos\beta_s)\operatorname{ctg}\beta_1 + \\ + \frac{l^2}{t^2}\,\frac{(c_{N1}\sin\beta_s - c_{T1}\cos\beta_s)^2}{4\sin^2\beta_1},\end{aligned}\right. \tag{43}$$

$$\operatorname{ctg}\beta_2 = \operatorname{ctg}\beta_1 + \frac{l}{t}\,\frac{c_{N1}\sin\beta_s - c_{T1}\cos\beta_s}{2\sin^2\beta_1}. \tag{44}$$

β_S is the angle between the blade chord (t-direction) and the cascade front (see Figure 7). The calculation of the pressure loss A_g from the pressure distribution can only make sense if we have a highly separated flow with an overbearing pressure resistance. It is then calculated from $A_g/q_1 = 1 - \Delta p/q_1 - q_2/q_1$.

3.4 Representation of Measurement Results Using Dimensionless Coefficients.

There are many ways of representing the experimental results of systematic cascade investigations because of the large number of parameters. A unified and clear form is especially desirable. We can formulate two requirements, that is,:

1. The representation should have a universal character, and should consider the deeper physical relationships.

2. The representation should allow one to derive the parameters required for the design of a blade cascade without complicated recalculations. It also should be possible to find the optimum cascade configuration for a certain task in a simple manner.

We should stress here that research in this area is not yet sufficient to uniquely select parameters which will characterize the cascade. In this sense, the following discussion is an attempt to clarify this problem using numerous contributions taken from the literature (see [2], [4], [9], [15]).

From a physical point of view, cascade flow must be considered as a superposition of a purely circulatory flow with a vortex intensity Γ which is arranged periodically along a straight line, and a translation flow w_∞. According to the Kutta-Joukowski theorem, a lift forces is produced perpendicular to the translation flow. If we consider the viscosity effect, there is also a drag force parallel to the translation flow. The important independent variable required to specify the direction of w_∞ is the angle between the translation flow and the blade chord, and it will be called the angle of attack $\alpha_\infty = \beta_\infty - \beta_S$ in conformance with the notation usually used for a single airfoil. We can now represent the lift coefficient as a function of the angle of attack

$$c_A = \frac{A}{\varrho w_\infty^2 l/2} = f(\alpha_\infty) \tag{45}$$

and the drag coefficient as a function of the lift coefficient

$$c_W = \frac{W}{\varrho w_\infty^2 l/2} = f(c_A) \tag{46}$$

to characterize the cascade flow. We find the well-known diagrams for the lift increase and the profile polars. In the range of healthy flow, the functional relationships of equations (45) can be represented by the linear function

$$c_A = \frac{dc_A}{d\alpha_\infty}(\alpha_\infty - \alpha_0) \tag{47}$$

where the constant lift increase $dc_A/d\alpha_\infty$ and the constant zero lift direction α_0 appear. This representation allows one to make the transition to a single airfoil, so that we can make comparisons with flows over single profiles. However, the relationship with the parameters which are important for designing the cascade such as pressure gradient, deflection and pressure loss, are relatively complicated. There is also the disadvantage that the lift coefficient contains part of the drag,

as can be seen from equations (24) and (25), so that sometimes rather unclear relationships are derived.

If we consider the blade cascade more from the point of view of technical applications, then one characteristic feature of cascade flow is the deflection of the incoming translational flow, and either a pressure increase or a pressure drop result. The circumferential component w_{1n} is looked upon as an independent variable for specifying the incoming flow, similar to the angle of attack α_∞. First, we will use the deflection $\Delta w_u = w_{2u} - w_{1u}$ as the "useful component" to characterize the flow state and later on, we will use the total pressure loss $\Delta g = g_1 - g_2$ as the "damaging component". We believe that the velocity normal to the cascade front w_a is especially well-suited when introducing dimensionless variables, because it determines the throughput through the cascade. Even if there are several cascades (stages), it remains almost constant. The cascade properties are represented by the deflection coefficients as a function of the circumferential component of the incident flow

$$\delta_a = \frac{\Delta w_u}{w_a} = f\left(\frac{w_{1u}}{w_a}\right) = f(\operatorname{ctg}\beta_1) \tag{48}$$

and by the loss coefficient as a function of the cascade deflection,

$$\zeta_{V_a} = \frac{\Delta g}{\varrho w_a^2/2} = f(\delta_a) \tag{49}$$

The first relationship is analogous to the lift increase given by equation (45). The second relationship is called the cascade polar*, similar to the profile polar given by equation (46). This last representation is especially important as we will show. The coefficients defined above have the advantage that they are in direct relationship with the velocity triangle of the cascade and give the energy loss of the flow**.

---

*The term "polar" only applies in the transferred sense.

**Here, we should realize that it is advantageous to use the cotangent of angles instead of the flow angles in degrees, when applied to cascades, because then these will always represent the circumferential component of the flow for the throughput "1". However, clarity is not lost if we become accustomed to this method of operation.

Instead of the deflection Δw_n, we could also use the pressure difference in the cascade $\Delta p = p_2 - p_1$ as the "useful component", but this quantity has the disadvantage that it contains the pressure loss in the cascade. /326

In the range of healthy and non-separated flow, we can describe the relationship between the deflection coefficient and the incident flow direction according to equation (45) using the following equation for a straight line:

$$\delta_a = A \operatorname{ctg} \beta_1 + B. \tag{50}$$

This relationship naturally follows from the basic equations of blade cascade flow (see Appendix F). The constants A and B depend on the lift increase and the zero-lift direction, similar to equation (47). Equation (50) has a practical meaning if it is possible to find a relationship between the constants A and B, and geometric profile parameters which have general validity, which seems to be a good possibility. At the present time, it does not seem likely that it will be possible to find a similar theoretical trial solution for the dependence of the loss coefficient on the deflection, according to equation (49), because the flow losses depend on the deflection in a very complicated way, because of the complicated processes in the friction layer of the blade profile. The coefficients defined by equations (48) and (49) are related to the flow angles by the relationship

$$\delta_a = \operatorname{ctg} \beta_2 - \operatorname{ctg} \beta_1 \tag{51}$$

and with the static pressure difference in the cascade by

$$\frac{p_2 - p_1}{\varrho w_a^2/2} = \operatorname{ctg}^2 \beta_2 - \operatorname{ctg}^2 \beta_1 + \zeta_{Va} \tag{52}$$

from the Euler turbine equation, we then find the lifting height of a blade cascade which is rotating at a velocity u

$$H = \frac{1}{g} w_a \left(u \delta_a - \frac{1}{2} w_a \zeta_{Va} \right). \tag{53}$$

One of the most important problems is the question of the optimum cascade configuration. By this, we mean the cascade configuration (t/l and β_s) for a given profile shape which results in a specified velocity

triangle with the lowest flow losses. For a specified velocity triangle, we can select the various division ratios t/l, which corresponds to a certain value of the blade angle β_s to achieve the specified outflow direction and a certain total pressure loss. If in a plane δ_3 and β_1, we plot the optimum values of t/l and β_s, corresponding to each pair of values, then we obtain an optimum characteristic field for the corresponding blade profile from which we can read off the optimum cascade configuration (t/l and β_s) for a specified velocity triangle (β_1 and δ_3). In this field the lines with equal minimum loss coefficients $\zeta_{Va\ min}$ can be plotted, so that all variables required for designing the cascade are contained in this characteristic field. Such a characteristic field, therefore, summarizes all of the cascade measurements for a certain blade profile and always contains the most favorable experimental points. One then plots the deflection and the loss as a function of the incident flow direction with fixed cascade geometry only to evaluate the blade cascade for incident flow conditions which are different from the design point. Of course this characteristic field says nothing about whether the profile shape used is the optimum one for the velocity triangle. By comparing the optimum characteristic fields of several profile shapes, it is possible to immediately decide the question of the most favorable profile shape, if one selects the profile shape for the specified velocity triangle for which the flow loss is the smallest.*

The representation of the cascade polar $\zeta_{Va} = f(\delta_a)$ given above is especially well-suited to determine the optimum cascade configuration. A fixed pair of values t/l and β_s corresponds to a cascade polar. If, for the same β_s we plot all of the cascade polars with various t/l above one another (Figure 14), then if there is a small deflection the curves with the largest division ratio will show the smallest loss. As the deflection is increased, however, the flow separates a large division ratio earlier than for a small division ratio, so that the curves with small division ratio have smaller losses. The envelope with all polars with various t/l then results in the minimum loss which corresponds to a single deflection and the tangential cascade polar gives the

*Just like the optimum cascade characteristic field problem for the minimum losses (efficiencies discussed here), optimum characteristic fields can also be designed for other minimum requirements, for example the maximum overvelocity over the profile (cavitation, critical Mach number or minimum shock sensitivity (steepness)).

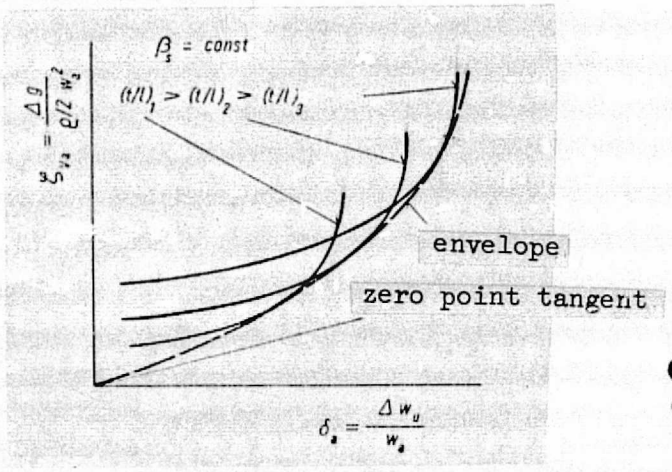

Figure 14: Determination of optimum cascade configuration using cascade polars.

corresponding optimum t/l value. In this way, the optimum value pairs t/l and β_s are obtained for a δ_3 value. The β_1 values corresponding to δ_3 are taken from a plot of δ_3 versus β_1. In order to draw the envelope, it is useful to know its tangent at the origin; that is, at t/l = ∞. The following formula can be given for this (see appendix G):

$$\left(\frac{\delta_3}{\zeta_{Va}}\right)_{t/l=\infty} = \frac{1}{2}\sin^2(\beta_s + \alpha_\infty)\left[\left(\frac{c_A}{c_W}\right)_{opt} - \operatorname{ctg}(\beta_s + \alpha_\infty)\right]. \tag{54}$$

In order to determine it, one requires the optimum quality coefficient of the single profile $c_A/c_W)_{opt}$ and the corresponding angle of attack α_∞. Using plots at various β_s values, we can finally find sufficient numbers of optimum values to obtain an optimum characteristic field*. /327

*Strictly speaking, in order to determine the optimum values, one should use cascade polars for fixed β_1 and t/l instead of for fixed β_s and t/l. For specified β_s, two cascade configurations will not have exactly the same velocity triangle for the same δ_3, but the values of β_1 and β_2 will be somewhat diffferent, because the incident flow angle depends on the division ratio. However, this has a very small influence on the optimum value determination. On the other hand, the suggestion method has the advantage of great simplicity, because the cascade geometry will remain constant for any one cascade polar.

4. SOME SYSTEMATIC MEASUREMENT RESULTS OF BLADE CASCADES WITH PROFILES NACA 0010* .

Out of the numerous systematic tests of blade cascade measurements which were performed at the Braunschweig Institute of Technology at the Fluid Mechanics Institute using the previously-described cascade test stand (see also [21], [23], [24]), we will, in the following, give a small selection of measurement results in order to demonstrate the evaluation methods.

These are blade cascades which are built up from symmetric profiles with the NACA system, having a 10% relative thickness (profile NACA 0010) The blade chord was $l = 200$ mm, and the exit velocity was about $w_2 = 40$ m/s, according to a Reynolds number of $Re = 5 \times 10^5$.

In addition to the values of the division ratio t/l, the blade angle β_s and the incident flow angle β_1 given by the experiment configuration, the measurement gives the average total pressure loss G obtained from an averaging process, the average pressure difference in the cascade P and the average departing flow angle β_{2y}. The numerical values given in columns 4 to 6 were measured at relatively large distances of 100 mm at $\beta_s = 90°$ and 130 mm at $\beta_s = 45°$ behind the blade cascade. Consequently, the wake valley is already relatively flat. Nevertheless, we find considerable deviations in the homogeneous outlet flow (columns 10 to 12) compared to the average values in the measurement plane (columns 4 to 6), especially in the valleys of the total pressure loss and in the static pressure difference. There are substantial deviations in the angles only for very small outlet flow angles. The quantities in parentheses in columns 10-12 which were all obtained from the complete evaluation formulas with variable β_{2y} (see appendix A) show almost complete agreement with the values of the approximate calculation. The parameter α of the valley shape (column 7) can also /328 be directly found from measurement results. The two constants K and κ (columns 8 and 9) were taken from universal diagrams (Figures 9 and 12). The contraction function κ was selected as $\kappa = 0.9$ in all examples, which means that the lift center of gravity of a blade was about 1/3 of the blade chord. In the contraction coefficients (columns 13 to 15), we find that the total contraction μ_{ges} is found directly from the re-

*The complete results will be published in later papers because they are very extensive.

Table 3: Evaluation scheme for wake measurement on blade cascades (numerical values for blade cascades with NACA 0010 profiles). The equation numbers refer to the equations in the text. The numbers in brackets in columns 10-12 are obtained from complete evaluation formulas with the variables β_{2y}.

	1	2	3	4	5	6	7	8	9
	t/l	β_1	β'_1	G	P	β_{2y}	a	K	κ
	specified			from wake measurement				universal	
	—		—	Eq (7)	Eq (8)	—	Eq (15)	Eq (17)	Eq (35)
a	1,00	90°	90°	0,0150	−0,0728	90,0°	0,627	0,0011	0,90
b	0,75	90°	90°	0,0215	−0,0637	90,0°	0,601	0,0017	0,90
c	0,50	90°	90°	0,0397	−0,0784	90,0°	0,556	0,0034	0,90
d	1,00	45°	45°	0,0175	−0,1332	43,0°	0,771	0,0007	0,90
e	0,75	45°	45°	0,0280	−0,1948	42,3°	0,759	0,0011	0,90
f	0,50	45°	45°	0,0507	−0,2214	41,0°	0,718	0,0021	0,90
	10	11	12	13	14	15	16	17	18
	l_g/q_1	l_p/q_1	β'_2	μ_{ges}	μ_I	μ_A	l_g/q_{1kor}	l_{pkor}/q_{1kor}	β_{2kor}
	homogeneous flow			contraction coefficients			corrected homogeneous outflow		
	Eq (10)	Eq (11)	Eq (13)	Eq (36)	Eq (37)	Eq (38)	Eq (27) to (30)		Eq (34)
a	0,0139 (0,0138)	−0,0706 (−0,0706)	90,0° (90,0°)	1,029	1,026	1,003	0,0131	−0,0131	90,0°
b	0,0198 (0,0198)	−0,0603 (−0,0604)	90,0° (90,0°)	1,020	1,018	1,002	0,0190	−0,0190	90,0°
c	0,0363 (0,0365)	−0,0716 (−0,0718)	90,0° (90,0°)	1,018	1,016	1,002	0,0351	−0,0351	90,0°
d	0,0168 (0,0168)	−0,1325 (−0,1325)	43,0° (43,0°)	1,019	1,017	1,002	0,0162	−0,0902	42,9°
e	0,0269 (0,0271)	−0,1938 (−0,1940)	42,3° (42,3°)	1,019	1,017	1,002	0,0260	−0,1489	42,2°
f	0,0485 (0,0483)	−0,2195 (−0,2198	41,0° (41,0°)	1,044	1,040	1,004	0,0446	−0,1289	40,8°

sults of the homogeneous outlet flow. The inlet contraction μ_E is determined using the value μ of the contraction function. The remaining part of the jet contraction is the exit contraction μ_A*. In these

*If, due to jet contractions, there is a substantial change in the outlet flow angle β_2, then it may be necessary to calculate it with the corrected outflow angle β_{2kor} and then find an improved contraction coefficient μ_{ges} in order to make the values of the corrected homogeneous outlet flow compatible with the plane continuity equation.

cases, we find jet contractions between 2 and 4%. However, it is easy for higher jet contractions to occur, especially when there are pressure increases. Accordingly, the corrections caused by jet contraction are relatively small (columns 16 to 18), but they are not negligible. As an example for the pressure distribution measurements, Figure 15 shows pressure distributions for the not-lined-up cascade with profiles NACA 0010 with three division ratios. The plot shows the uncorrected that is, the directly-measured measurement points and the measurement points which have been corrected using equation (39), as well as a pressure distribution of the potential theory of H. Schlichting [21]. The corresponding contraction coefficients can be found in Table 3 (columns 1 to 3). The corrected values agree quite well with theory, even though deviations are found for very small division ratios which could partially be caused by friction.

The results of the wake measurement will be represented as profile values (equation (45) and (46)), as well as cascade values [equation (48), (49)). Figure 16 shows the lift increase c_A plotted against

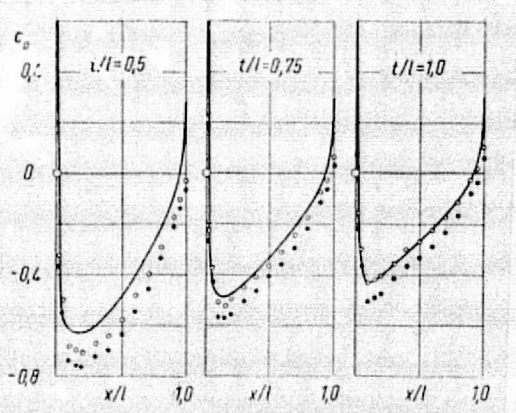

Figure 15: Pressure distribution for NACA 0010 profiles in a cascade not lined up with incident flow parallel to the chord (β_s = = β_1 = 90°).

● - uncorrected measurement
O - corrected measurement.

α_∞, which depends greatly on the division as well as whether the blades are lined up. Figure 17 shows the corresponding plot of the cascade values δ_a as a function of ctg β_1. The plot agrees very well with the

form of equation (50). It is also remarkable that the inclination of the line (constant A) depends hardly at all on the division, and only slightly on how much the blades are lined up. The origin displacement (constant B) depends on the zero-lift direction, and therefore also on the division and how the blades are lined up.

The profile polars calculated from the wake measurements are given in Figure 18. As the division is refined, the drag in general increases because of the less favorable pressure distribution (higher overvelocities) and the maximum lift decreases. The difference between the pumping cascades and the turbine cascades is clearly seen for the lined-up cascade by the assymetry with respect to $c_A = 0$. On the turbine side ($c_A > 0$), substantially higher c_A values are reached. Figure 19 contains a plot of the cascade polars $\zeta_{Va}(\delta_a)$ which is similar. The characteristic feature of this plot was already discussed in the previous section (see Figure 14). Inorder to determine the optimum cascade configuration, we use the envelopes of cascade polars for various division ratios t/l. The tangents of the envelopes at the origin ($t/l \to \infty$) can be calculated from equation (54), and in the previous example we will use an optimum quality coefficient of a single profile of $(c_A/c_W)_{opt} = 60$ at $\alpha_\infty = 10^0$. These results and further results for other blade angles β_s allow one to design an optimum cascade characteristic field using the optimum values obtained, and this is shown in Figure 20 for blade cascades made up of NACA 0010 profiles. The characteristic field contains in a plane of deflection coefficient, δ_a versus incident flow direction ctg β_1, the lines of the optimum values of the division ratio t/l and of the blade angle β_s. This means that for a specified velocity triangle, one can read off the most favorable cascade configuration. As to be expected, the characteristic field shows that in the pumping cascade region, the optimum division ratios are substantially lower than in the turbine cascade region. The corresponding loss coefficients are greater in the pumping cascade region. Of course, we can only use points of the characteristic fields for this comparison which are on the pump side or the turbine side, and whose corresponding velocity triangles are derived from each other by reversing the flow direction (exchange of w_1 and w_2). For such points, we have the relationship

$$(\mathrm{ctg}\,\beta_1)_{\mathrm{Turbine}} = -(\mathrm{ctg}\,\beta_1)_{\mathrm{Pump}} - \delta_a.$$

The corresponding points are therefore not symmetric with respect to ctg $\beta_1 = 0$, but are displaced toward the pump side, similar to the curve $\beta_s = \text{const}$.

5. OUTLOOK

For a very long time, the Euler stream thread theory was the only method of analyzing the very complex blade cascade flows. In recent times, several new directions of research have emerged, which can be characterized as follows:

Starting with the Euler stream thread theory, which describes the limiting case of very thin and infinitely dense blades with friction-less flow, an attempt was made to develop a reduced performance theory which describes the deviations with respect to the blade-congruent flow by means of universal and empirical relationships (A. Betz, Goettingen). As a second method, the extensively-researched flow around a single

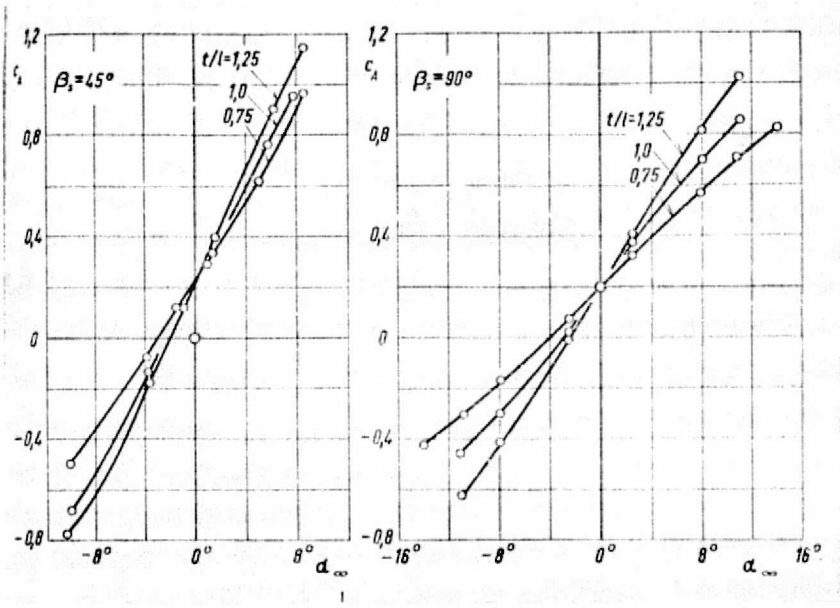

Figure 16: c_A as a function of α_∞ for NACA 0010 profiles in a cascade not lined up ($\beta_s = 90°$) and lined up ($\beta_s = 45°$).

profile was used as a point of departure, and an attempt was made to approximate the deviations due to the cascade configuration of the blades (A. Betz, Goettingen). Both methods depart relatively far /330 from the point of departure, in the division ratio region of about

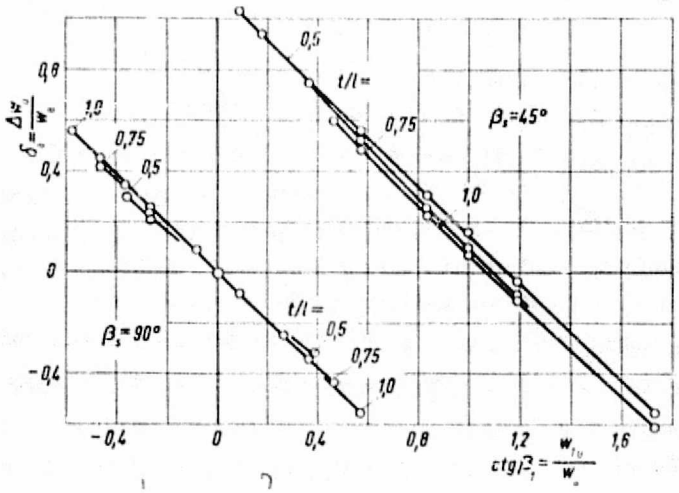

Figure 17: δ_a as a function of ctg β_1 for blade cascades with NACA 0010 profiles, not lined up (β_s = 90°) and lined up (β_s = 45°).

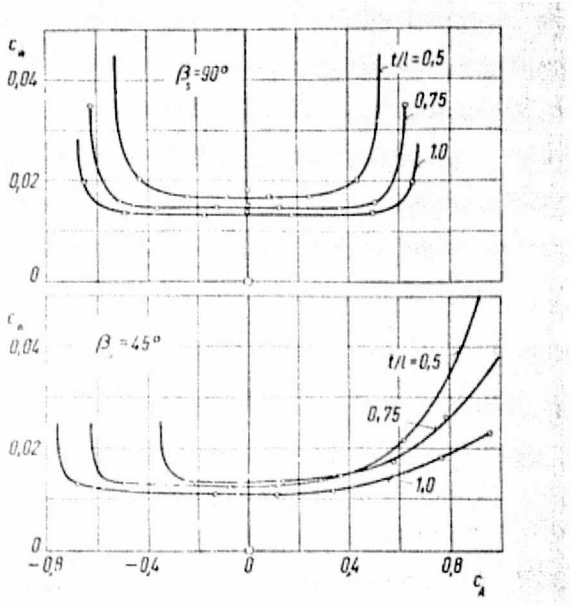

Figure 18: Profile polars for NACA 0010 profiles in a cascade, not lined up (β_s = 90°), and lined up (β_s = 45°).

t/l = 1 and therefore the uncertainties become quite substantial. Because of the continuous development of the aircraft gas turbines, especially in England during the last war, blade cascade flows were calculated extensively using empirical methods. An attempt was made to develop generally valid empirical relationships for the design of gas turbines (A. R. Howell, Farnborough). Because of the successes of boundary layer methods in the layer of aircraft dynamics, recently an attempt was made to give a boundary layer treatment of the plane blade

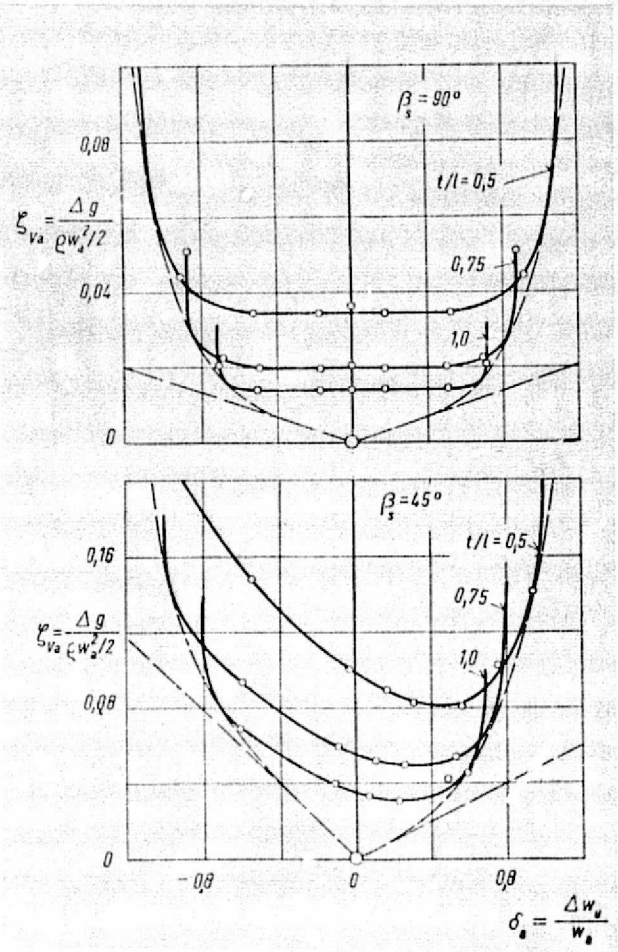

Figure 19: Cascade polars for blade cascades with NACA 0010 profiles, not lined up (β_s = 90°) and lined up (β_s = 45°).

cascade flow in its complete generality ((H. Schlichting, Braunschweig). For the first time, it was possible to calculate theoretically a blade cascade flow with friction, and good agreement with the experiment was obtained.

This last method which is the topic of our investigation will support experimental research for the purpose of validating the reliability of the theoretical results with respect to several important points of the entire field. This will lead to a substantial reduction in the experimental effort. Measurement results are very important for comparisons between theory and experiment. As the previous discussion shows, achieving a sufficiently two-dimensional flow, recalculating the measurement results for a homogeneous flow, and the correction of the measurement results with respect to the remaining jet contraction, are all-important factors which have not been considered enough before.

All of the research discussed above is concerned with two-dimensional

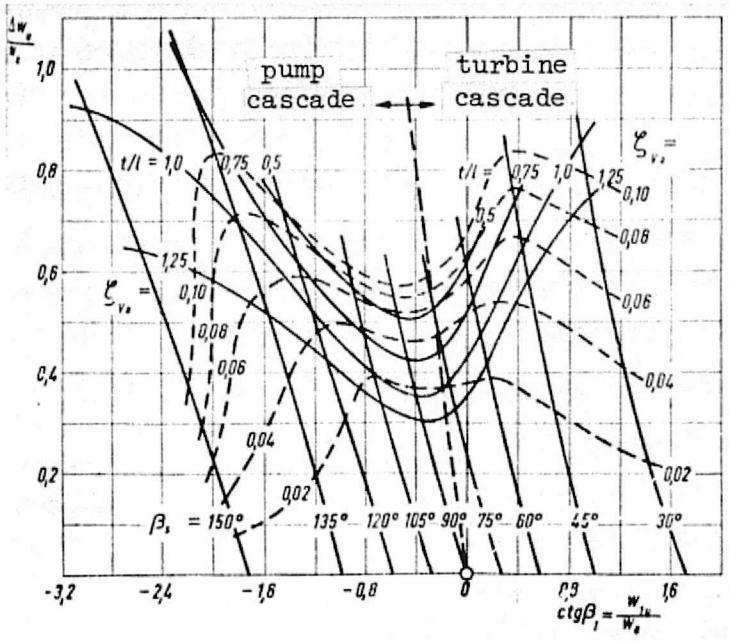

Figure 20: Optimum cascade characteristic field for blade cascades with NACA 0010 profiles.

plane flow through an infinitely-long blade cascade. Certainly, this flow is the foundation of any cascade flow. However, it has been recognized that there are very different three-dimensional influences which occur in a designed flow machine, and this can result in substantial differences with respect to the plane cascade flow. Nevertheless, the influences, must be considered as secondary phenomena in the sense of analyzing the cascade flows, and they must be dealt with separately. Even though important contributions have been made to these solutions in several special cases, a rational analysis of these problems remains to be done.

6. APPENDIX

A. Equations for the homogeneous flow behind a blade cascade with consideration of the variability of β_{2y}.

If we consider the variability of the outflow angle β_{2y}, with the cascade parallel coordinate y, we find the following from equations (1) to (3):

$$w_2^2 = w_{2a}^2 + w_{2n}^2 = \left(\frac{1}{t}\int_y^{y+t} w_2(y)\sin\beta_{2y}(y)\,dy\right)^2 + \left(\frac{1}{t}\int_y^{y+t} w_2^2(y)\sin\beta_{2y}(y)\cos\beta_{2y}(y)\,dy\right)^2 + \left(\frac{1}{t}\int_y^{y+t} w_2(y)\sin\beta_{2y}(y)\,dy\right)^2, \tag{A-1}$$

$$p_2 = \frac{1}{t}\int_y^{y+t} p_2(y)\,dy + \varrho\,\frac{1}{t}\int_y^{y+t} w_2^2(y)\sin^2\beta_{2y}(y)\,dy - \varrho\left(\frac{1}{t}\int_y^{y+t} w_2(y)\sin\beta_{2y}(y)\,dy\right)^2, \tag{A-2}$$

$$\operatorname{ctg}\beta_2 = \frac{\frac{1}{t}\int_y^{y+t} w_2^2(y)\sin\beta_{2y}(y)\cos\beta_{2y}(y)\,dy}{\left(\frac{1}{t}\int_y^{y+t} w_2(y)\sin\beta_{2y}(y)\,dy\right)^2}. \tag{A-3}$$

B. Determination of the homogeneous outflow from the average values of the inhomogeneous flow.

Equation (4) for the square of the velocity of the outflow velocity w_2 can be written as follows by using equation (9):

$$\frac{w_2^2}{w_1^2} = \sin^2\beta_{2y}\left(\frac{1}{t}\int_y^{y+t}\frac{w_2^2(y)}{w_1^2}\,dy - K\right) + \cos^2\beta_{2y}\left(\frac{\left(\frac{1}{t}\int_y^{y+t}\frac{w_2^2(y)}{w_1^2}\,dy\right)^2}{\frac{1}{t}\int_y^{y+t}\frac{w_2^2(y)}{w_1^2}\,dy - K}\right). \tag{B-1}$$

The second term can be simplified as follows, because K is small compared with the integral in the denominator:

$$\frac{w_2^2}{w_1^2} = \sin^2\beta_{2y}\left(\frac{1}{t}\int_y^{y+t}\frac{w_2^2(y)}{w_1^2}\,dy - K\right) + \cos^2\beta_{2y}\left(\frac{1}{t}\int_y^{y+t}\frac{w_2^2(y)}{w_1^2}\,dy + K\right). \tag{B-2}$$

If we consider the identity

$$\frac{\varrho}{2}w_2^2(y) - \frac{\varrho}{2}w_1^2 = [g_1 - g_2(y)] - [p_2(y) - p_1], \tag{B-3}$$

then from equation (B - 2) we obtain equation (12) as follows by introducing the integral values G and P using equations (7) and (8):

$$\frac{w_2^2}{w_1^2} = \frac{q_2}{q_1} = 1 - G - P - K \sin^2 \beta_{2y} + K \cos^2 \beta_{2y}. \tag{B-4}$$

Equation (5) for the static pressure p_2 can be transformed to the form of equation (11) which can easily be seen by introducing the quantity /331 K according to equation (9):

$$\frac{p_2 - p_1}{q_1} = \frac{\Delta p}{q_1} = P + 2K \sin^2 \beta_{2y}. \tag{B-5}$$

The total pressure loss can be expressed using the identity similar to equation (B-3):

$$\frac{g_1 - g_2}{q_1} = 1 - \frac{p_2 - p_1}{q_1} - \frac{q_2}{q_1} \tag{B-6}$$

and by equation (B-4) and (B-5):

$$\begin{aligned} \frac{g_1 - g_2}{q_1} = \frac{\Delta g}{q_1} &= 1 - P - 2K \sin^2 \beta_{2y} - \\ &= 1 - G - P + K \sin^2 \beta_{2y} - K \cos^2 \beta_{2y}. \end{aligned} \tag{B-7}$$

From this, we obtain the desired relationship, equation (10):

$$\frac{\Delta g}{q_1} = G - K. \tag{B=8}$$

Equation (6) for the outflow angle β_2 can be written as follows, using equation (9):

$$\operatorname{ctg} \beta_2 = \operatorname{ctg} \beta_{2y} \frac{\frac{1}{t} \int_y^{y+t} \frac{w_2^2(y)}{w_1^2} dy}{\frac{1}{t} \int_y^{y+t} \frac{w_2^2(y)}{w_1^2} dy - K}. \tag{B-9}$$

Since the correction term K is small compared to the integral in the

denominator, equation (B-9) can be further simplified as:

$$\operatorname{ctg}\beta_2 = \operatorname{ctg}\beta_{2y}\left\{1 + \frac{K}{\frac{1}{t}\int_{y}^{y+t}\frac{w_2^2(y)}{w_1^2}\,dy}\right\}.$$

The integral in the denominator can be expressed by the integral value G and P using equations (7) and (8), so that we obtain equation (13):

$$\operatorname{ctg}\beta_2 = \operatorname{ctg}\beta_{2y}\left(1 + \frac{K}{1-P-G}\right). \tag{B-10}$$

C. Universal Calculation of the Correction term K using correction term using equation (9).

If we introduce the trial solution for the velocity value equation (14) where w_{2max} is dimensionless, then using equation (15),

$$\frac{w_2(\eta)}{w_{2\max}} = 1 - (1-\sqrt{a})\,e^{-c\eta^2}. \tag{C-1}$$

the integration of equation (C-1) between $-\infty$ and ∞ gives

$$\int_{-\infty}^{+\infty}\frac{w_2(\eta)}{w_{2\max}}\,d\eta = 1 - \sqrt{\pi}(1-\sqrt{a})\,\frac{1}{c}. \tag{C-2}$$

Since we have assumed that the wake valley has already practically decayed to zero, in the range of one blade division ($-1/2 < \eta < 1/2$), then the value of the integral field remains unchanged, if we only integrate over the range from -1/2 to 1/2. Correspondingly we obtain the following for the value of the velocity square (stagnation pressure valley):

$$\int_{-\infty}^{+\infty}\frac{w_2^2(\eta)}{w_{2\max}^2}\,d\eta = 1 - 2\sqrt{\pi}(1-\sqrt{a})\,\frac{1}{c} + \sqrt{\frac{\pi}{2}}(1-\sqrt{a})^2\,\frac{1}{c}. \tag{C-3}$$

From equation (C-3), we can then determine the undetermined parameter C by the area of the stagnation pressure valley. By using the identiy (B-3),

$$\int_{-1/2}^{+1/2} \frac{w_2^2(\eta)}{w_{2\max}^2}\, d\eta = \int_{-1/2}^{+1/2} \frac{q_2(\eta)}{q_{2\max}}\, d\eta =$$

$$= \frac{q_1}{q_{2\max}} \int_{-1/2}^{+1/2} \frac{q_1 - (g_1 - g_2(\eta)) - (p_2(\eta) - p_1)}{q_1}\, d\eta. \qquad \text{(C-4)}$$

From this, by introducing the integral values (7) and (8):

$$\int_{-1/2}^{+1/2} \frac{w_2^2(\eta)}{w_{2\max}^2}\, d\eta = \frac{q_1}{q_{2\max}} (1 - P - G). \qquad \text{(C-5)}$$

Since the flow outside of the wake valley has no losses with $q_2(\eta) = q_{2max}$, and also because q_{2max} and therefore also the static pressure p_2 can be assumed to be constant over the division, we obtain:

$$\frac{q_{2\max}}{q_1} = \frac{q_1 - (p_2 - p_1)}{q_1} = 1 - P. \qquad \text{(C-6)}$$

By introducing equation (C-5) and (C-6) for the right side of equation (C-3), we then find equation (16) for the parameter c:

$$c = \left[2 \left| \pi (1 - \left| a) - \right| \frac{\pi}{2} (1 - \sqrt{a})^2 \right] \frac{1 - P}{G}. \qquad \text{(C-7)}$$

The correction term of equation (9) can be written as:

$$K = \frac{q_{2\max}}{q_1} \left[\int_{-1/2}^{+1/2} \frac{w_2^2(\eta)}{w_{2\max}^2}\, d\eta - \left(\int_{-1/2}^{+1/2} \frac{w_2(\eta)}{w_{2\max}}\, d\eta \right)^2 \right]. \qquad \text{(C-8)}$$

From this, we can first find the following by introducing equation (C-2) and (C-3) for the integrals and equation (15) for the factor in front of the bracket:

$$K = (1 - P) \left(\left| \frac{\pi}{2} (1 - \left| a)^2 \frac{1}{c} - \pi (1 - \sqrt{a})^2 \frac{1}{c^2} \right). \right. \qquad \text{(C-9)}$$

If for the parameter c we will introduce the equation (C-7), then after

conversion we find the desired relationship (7):

$$K_G = \frac{(1 - \lambda_2 a) - \frac{2}{2\lambda_2 2} - (1 - \lambda_2 a)\frac{G}{1 - P}}{2\lambda_2 2 \quad (1 - \lambda_2 a)}. \tag{C-10}$$

D. Derivation of the formula for the outflow angle correction.

If in the equation for the incoming and outgoing momenta $I_E + I = I_A$ we substitute (31), (32), and (33), we obtain:

$$\begin{cases} \varrho Q_G w_{2\,\mathrm{kor}} \cos\beta_{2\,\mathrm{kor}} + \\ \quad + \varrho (Q_2 - Q_G) \frac{1}{2} (w_{2\,\mathrm{kor}} \cos\beta_{2\,\mathrm{kor}} + \\ \quad\quad + w_2 \cos\beta_2) = \varrho Q_2 w_2 \cos\beta_{2\,\mathrm{kor}}. \end{cases} \tag{D-1}$$

After conversion, we find /332

$$\begin{cases} Q_G (w_{2\,\mathrm{kor}} \cos\beta_{2\,\mathrm{kor}} - w_2 \cos\beta_2) = \\ \quad = Q_2 (w_2 \cos\beta_2 - w_{2\,\mathrm{kor}} \cos\beta_2). \end{cases} \tag{D-2}$$

Because of continuity,

$$\begin{cases} Q_G = t\, w_{2\,\mathrm{kor}} \sin\beta_{2\,\mathrm{kor}}, \\ Q_2 = t\, w_2 \sin\beta_2. \end{cases} \tag{D-3}$$

If we introduce Q_2 and Q_G instead of the velocities w_{2kor} and w_2 in equation (D-2), then we find:

$$\begin{cases} Q_G^2 \operatorname{ctg}\beta_{2\,\mathrm{kor}} + Q_2 Q_G \operatorname{ctg}\beta_{2\,\mathrm{kor}} = \\ \quad = Q_2^2 \operatorname{ctg}\beta_2 + Q_G Q_2 \operatorname{ctg}\beta_2. \end{cases} \tag{D-4}$$

This gives us the desired result:

$$\operatorname{ctg}\beta_{2\,\mathrm{kor}} = \frac{Q_2}{Q_G} \operatorname{ctg}\beta_2. \tag{D-5}$$

E. Determination of the Homogeneous Outflow from the Pressure Distribution at the Blade Contour.

From the forced composition, we first find the following relationships from the coefficients c_N and c_T and c_U and c_S on the other hand, (all referred to w_∞)

$$c_U = c_N \sin\beta_\infty - c_T \cos\beta_\infty, \tag{E-1}$$

$$c_S = -c_N \cos\beta_\infty - c_T \sin\beta_\infty. \tag{E-2}$$

Angles are given in Figure 4, and signs of the forces are given in footnotes in the previous sections.

From the momentum theorem, in the circumferential direction (see equation (21), we find the outlet flow angle

$$\operatorname{ctg}\beta_2 = \operatorname{ctg}\beta_1 + \frac{l}{t}\frac{c_U}{2\sin^2\beta_\infty}, \tag{E-3}$$

and after introducing equation (E-1) and the coefficients c_{N_1} and c_{T_1} referred to w_1,

$$\operatorname{ctg}\beta_2 = \operatorname{ctg}\beta_1 + \frac{l}{t}\frac{c_{N1}\sin\beta_\infty - c_{T1}\cos\beta_\infty}{2\sin^2\beta_1}, \tag{E-4}$$

so that we obtain an equation (44). From the momentum theorem in the axial direction, we find the following for the pressure difference in the cascade (see equation (22)):

$$\frac{p_2 - p_1}{q_1} = \frac{l}{t}\frac{\sin^2\beta_1}{\sin^2\beta} c_S, \tag{E-5}$$

After introducing equation (E-2), equation (42) gives

$$\frac{p_2 - p_1}{q_1} = -\frac{l}{t}(c_{N1}\cos\beta_\infty + c_{T1}\sin\beta_\infty). \tag{E-6}$$

According to the plane continuity equation, the stagnation pressure ratio can be expressed by the angles:

$$\frac{q_2}{q_1} = \frac{\sin^2\beta_1}{\sin^2\beta_2} = \sin^2\beta_1(1 + \operatorname{ctg}^2\beta_2). \tag{E-7}$$

If we substitute equation (E-4) for ctg β_1, then after further simplification we obtain equation (43):

$$\left\{\begin{aligned}\frac{q_2}{q_1} = 1 + \frac{l}{t}(c_{N1}\sin\beta_s - c_{T1}\cos\beta_s)\operatorname{ctg}\beta_1 + \\ + \frac{l^2}{t^2}\frac{(c_{N1}\sin\beta_s - c_{T1}\cos\beta_s)^2}{4\sin^2\beta_1}.\end{aligned}\right. \tag{E-8}$$

F. Derivation of a functional relationship between the deflection coefficient δ_3 and the incident flow angle β_1.

For a single profile, we find the relationship between the circulation and the angle of attack from

$$\Gamma_E = \pi w_\infty l \sin(\alpha_\infty - \alpha_0) \tag{F-1}$$

(α_0 = angle of attack for zero lift). If we use the same relationship for the blade profile in a cascade, and if we introduce the cascade influence factor $k = \Gamma_G/\Gamma_E$, then the circulation of the cascade blade is given by:

$$\left\{\begin{aligned}\Gamma_G = k\pi w_\infty l \sin(\alpha_\infty - \alpha_0) = \\ = k\pi w_\infty l \sin(\beta_\infty - \beta_0),\end{aligned}\right. \tag{F-2}$$

where w_∞ now is the vector average of w_1 and w_2. The angles β are not measured with respect to blade chord in contrast to the angles α, but are measured with respect to the cascade front used as a reference direction. Accordingly, β_0 is the incident flow angle of the cascade, for which the lift is zero.

We have the following relationship for the circumferential components of a cascade flow in front of and behind the cascade

$$w_{2u} = w_{1u} + \frac{\Gamma_G}{t}. \tag{F-3}$$

By substituting equation (F-2) and using $w_{ax} = w_\infty \sin\beta_\infty$, we find the following if the entire equation is divided by w_a:

$$\operatorname{ctg}\beta_2 = \operatorname{ctg}\beta_1 + k\pi\,\frac{l}{t}\,\frac{\sin(\beta_\infty - \beta_0)}{\sin\beta_\infty}. \tag{F-4}$$

For the angle β_∞, we have:

$$\operatorname{ctg}\beta_\infty = \tfrac{1}{2}(\operatorname{ctg}\beta_1 + \operatorname{ctg}\beta_2). \tag{F-5}$$

From equation (F-4) and by using the addition theorem and introducing equation (F-5), we immediately find:

$$\left\{\begin{aligned}\operatorname{ctg}\beta_2 = \operatorname{ctg}\beta_1 &+ k\pi\,\frac{l}{t}\cos\beta_0 - \\ &- k\,\frac{\pi}{2}\,\frac{l}{t}\sin\beta_0(\operatorname{ctg}\beta_1 + \operatorname{ctg}\beta_2)\end{aligned}\right. \tag{F-6}$$

An additional conversion gives:

$$\left\{\begin{aligned}&\operatorname{ctg}\beta_2 - \operatorname{ctg}\beta_1 = \delta_a = \\ &= \frac{k\pi\,\frac{l}{t}\sin\beta_0}{1 + k\,\frac{\pi}{2}\,\frac{l}{t}\sin\beta_0}\operatorname{ctg}\beta_1 + \frac{k\pi\,\frac{l}{t}\cos\beta_0}{1 + k\,\frac{\pi}{2}\,\frac{l}{t}\sin\beta_0}.\end{aligned}\right. \tag{F-7}$$

which is an equation of the form

$$\delta_a = A\operatorname{ctg}\beta_1 + B$$

with the constants

$$\left\{\begin{aligned}A &= -\frac{k\pi\,\frac{l}{t}\sin\beta_0}{1 + k\,\frac{\pi}{2}\,\frac{l}{t}\sin\beta_0}, \\ B &= \frac{k\pi\,\frac{l}{t}\cos\beta_0}{1 + k\,\frac{\pi}{2}\,\frac{l}{t}\sin\beta_0}.\end{aligned}\right. \tag{F-8}$$

/333

These constants only depend on the zero-lift direction of the cascade β_0 and the cascade influence factor k or the lift increase of the blade profile in the cascade.

G. Derivation of the formula for the limiting value of δ_a/ζ_{Va} for $t/l \to \infty$ (see [23]).

Using the expressions for c_A obtained using equations (24) and (25), we find:

$$\frac{c_W}{c_A} = \frac{1}{2} \sin^2 \beta_\infty \frac{\zeta_{Va}}{\delta_a} + \operatorname{ctg} \beta_\infty . \tag{G-1}$$

For a single profile, ($t/l \to \infty$), the optimum value of δ_a/ζ_{Va} is obtained when c_W/c_A is the minimum. Also, for a single profile we have

$$\beta_\infty = \beta_s + a_\infty , \tag{G-2}$$

so that the optimum value of δ_a/ζ_{Va} at $t/l \to \infty$ results in the following equation (54):

$$\left(\frac{\delta_a}{\zeta_{Va}} \right)_{t/l \to \infty} = \frac{1}{2} \sin^2 (\beta_s + a_\infty) \left[\left(\frac{c_A}{c_W} \right)_{opt} - \operatorname{ctg} (\beta_s + a_\infty) \right]. \tag{G-3}$$

REFERENCES

1. Christiani, K.: Experimental Investigation of an Air Foil in a Cascade Configuration, Luftfahrtforschung 2 (1928), p. 91-110.

2. Keller, C.: Axial Blower from the Point of View of Air Foil Theory, Dissertation E.T.H., Zurich, 1934.

3. Hausenblas, H.: Experiments with Turbine Blade Cascades, Ing.-Arch. 19 (1951), p. 75-82.

4. Sawyer, W. T.: Experimental investigation of a stationary cascade of aerodynamic profiles. Mitteilung d. Inst. f. Aerodynamik der E.T.H., Zurich, No. 17 (1949).

5. Blight, F. G., Howard, W., and McCallum, H.: The design and performance of a low-speed cascade tunnel. Dept. of Supply and Development, Div. of Aeronautics, Eng. Note No. 133 (1949).

6. Carter, A.D.S., Andrews, S. J., Shaw, H.: Some fluid dynamic research techniques. Inst. of Mech. Eng. Proc. 163, (1950), p. 249-263.

7. Mortarino, C.: Experiments of blades for compressors, Aerotechnica 30 (1950), p. 59-72.

8. Erwin, J. R., Emergy, J. C.: Effect of Tunnel Configuration and Testing Technique on Cascade Performance. NACA Rep. 1016, (1951).

9. Tranpel, W.: Neue allgemeine Theorie der mehrstufigen axialen Turbomashinen [New General Theory of Multi-Stage Axial Turbo Machines], Verlag Leeman and Co., Zurich, 1942.

10. Young, A. D.: Note on a method of measuring profile drag by means of an integrating comb. ARC R. & M., 2318 (1950).

11. Carter, A.D.S. and Cohen, E. M.: Preliminary investigation into a three-dimensional flow through a cascade of airfoils. ARC R. & M., 2339 (1949).

12. Hawthorne, W. R.: Induced deflection angle in Cascades. Journ. Aeron. Sci., 16 (1949), p. 252-253.

13. Tranpel, W.:Vortex systems in blade cascades and turbomachines. ZAMP 4 (1953), p. 298-311.

14. Katzoff, S., Bogdonoff, E. H., Boyet, H.: Comparison of theoretical and experimental lift and pressure distribution on airfoils in cascade. NACA TN 1388 (1947).

15. Zweifel, O.: The question of optimum blade division for blades of turbomachines, especially for large deflections in the blade rows. BBC-Mitteilungen 32 (1945), p. 436-444.

16. Schlichting, H., Scholz, N.: The determination of flow losses of a plane blade cascade. Ing.-Arch. 19 (1951), p. 42-65.

17. Howell, A. R.: The present basis of axial flow compressor design. ARC R. & M., 2095 (1942).

18. Scholz, N.: Two-dimensional correction of the outlet angle in cascade flow. Journ. Aeron. Sci., 20 (1953), p. 786-787.

19. Schlichting, H.: Results and Problems of Blade cascade investigations. Z. f. Flugwiss. I (1953), p. 109-122.

20. Schlichting, H.: Problems and results of investigations on cascade flow. Journ. Aeron. Sci. 21 (1954), p. 163-178.

21. Schlichting, H.: Calculation of frictionless incompressible flow for a specified plane blade cascade. VDI-Forschungsheft 447 (1955).

22. Scholz, N.: Application of the momentum theorem for measurements of blade cascades. ZAMM 34 (1954), p. 339-341.

23. Speidel, L.: Results of systematic investigation of blade cascades. Part IX. Calculation of the loss coefficients, Report 55/5 of the Inst. f. Strömungsmechanik der TH Braunschweig, (1955).

24. Scholz, N.: Investigations of blade cascades of flow machines. Z. f. Flugwiss. 3 (1955), p. 99-104.